Evaluation of polyunsaturated fatty acid uptake, distribution, and incorporation into specific muscle types

by

Payman Charkhzarin

A thesis
presented to the University of Waterloo
in fulfillment of the
thesis requirement for the degree of
Master of Science
in
Kinesiology

Waterloo, Ontario, Canada, 2009

AUTHOR'S DECLARATION

I hereby declare that I am the sole author of this thesis. This is a true copy of the thesis, including any required final revisions, as accepted by my examiners.

I understand that my thesis may be made electronically available to the public.

ABSTRACT

Polyunsaturated fatty acids (PUFA) affect key cellular and physiological processes in the body ranging from cell signalling to inflammation. Compositional, dietary refinement and bioassay studies have shown strong associations between the PUFA composition of skeletal muscle with various contractile properties as well as the development of obesity and insulin resistance. Relatively little is known about the uptake and incorporation of PUFA in skeletal muscle, especially in regards to fibre type-specific properties. The incorporation of PUFAs into rat soleus (slow-twitch oxidative), red gastrocnemius (fast-twitch oxidative), and white gastrocnemius (fast-twitch glycolytic) muscle were examined using stable isotope-labelled fatty acids and a novel internal isobutane positive chemical ionization (PCI) gas chromatography-mass spectrometry (GC-MS) technique. Two separate tracer studies were conducted. In the first study, four groups of rats were orally dosed by gavage with one of three isotopes of 18:2n-6; $^{13}C_{18}$-18:2n-6 ethyl ester, $^{13}C_{18}$-18:2n-6 nonesterified fatty acid or $^{2}H_{5}$-18:2n-6 ethyl ester and a control group received the vehicle only (olive oil). Animals were sacrificed 8 hours post dosing and soleus, red and white gastrocnemius muscles were collected for lipid analysis. In the second study, rats were orally administered a single dose of a mixture of 4 isotopes (0.15 mg/g body weight each of ethyl $^{13}C_{18}$-18:2n-6, ethyl $^{2}H_{5}$-18:3n-3, ethyl $^{13}C_{16}$-16:0, and nonesterified $^{2}H_{2}$-18:1n-9) or vehicle only (olive oil) as a control. Groups of animals were sacrificed at 8, 24, and 48 h after dosing and four muscle types (heart, soleus, red and white gastrocnemius) were collected and analyzed for isotopic signal of these fatty acids and their corresponding desaturation and/or elongation products. Soleus accumulated the most 18:2n-6 and 18:3n-3 followed by red gastrocnemius and white gastrocnemius. Soleus also accumulated significantly

higher concentrations of labelled n-6 fatty acids derived from 18:2n-6 in both studies. Heart muscle accumulated 20:5n-3 and 22:6n-3 increasingly over time while skeletal muscle accumulation was variable across fibre types. Labelled 20:5n-3 was detected in red and white gastrocnemius at 8 and 24 hr with levels declining by 48 h while no 20:5n-3 was detected in soleus at anytime. Labelled 22:6n-3 was not detected in white gastrocnemius, but 22:6n-3 appeared to be increasing in red gastrocnemius over time. Soleus demonstrated a large accumulation of 22:6n-3 at 8 h with no detectable levels at 48 h. In conclusion, we were able to demonstrate that the distribution and metabolism of various PUFAs differ in muscle types with distinct fibre type composition using a novel internal isobutane PCI GC MS method. Further research is warranted to examine discrepancies in PUFA accumulation in distinct muscle types.

ACKNOWLEDGEMENTS

The successful completion of this thesis would not have been possible without the support, generosity and hard work of a long list of people, to whom I will remain indebted. I am deeply indebted to my supervisor and mentor Dr. Ken Stark whose support, stimulating suggestions and encouragement helped me in all the time of research and writing of this thesis. I also acknowledge the assistance of my colleague and dear friend Hamid Izadi, without whose help this thesis would never have been completed. Adam Metherel, Ashley Patterson, and Alex Kitson have also greatly assisted me in the lab with virtually all aspects of my thesis work, and all have been dear friends. I thank Margaret Burnett for ensuring smooth daily operation in our lab and Dawn McCutcheon for her generous help with animal handling techniques. Deepest gratitude goes to Dr. Joe Quadrilatero and Dr. Russ Tupling for their abundant help and their invaluable assistance, support and guidance and access to their lab resources and years of friendship. I also thank Dr. Jim Rush for his overwhelming support, invaluable advices, bountiful access to his lab resources and years of companionship. My other colleagues in the Kinesiology department's physiology wing deserve mention for their assistance and friendship. These include Justin Chung, Steve Dennis, Chris Vigna, Eric Bombardier Rebecca Ford, Andrew Levi, and Andrew Robertson. Special thanks also to Ruth Gooding, executive secretary of the Kinesiology Department, for her ample assistance and guidance with the administrative work associated with this thesis. I wish to express my love and gratitude to my beloved family; Kameleh and Alijan Charkhzarin, for their understanding and endless love, through the duration of my studies. And finally, I am thankful for the significant public funds that I have received to complete my thesis.

TABLE OF CONTENTS

LIST OF FIGURES

LIST OF TABLES

LIST OF ABBREVIATIONS

AA	Arachidonic acid, 20:4n-6
ALA	Alpha-linolenic acid, 18:3n-3
BF_3	Boron trifluoride
CI	Chemical ionization
C-IRMS	Combustion isotope ratio mass spectrometry
CPTI	Carnitine palmitoyl transferases I
DHA	Docosahexaenoic acid, 22:6n-3
EDL	Extensor digitorum longus
EE	Ethyl ester
EFAD	Essential fatty acid deficient
EI	Electron ionization
EPA	Eicosapentaenoic acid
FABPpm	Fatty acid binding protein pm
FAME	Fatty acid methyl ester
FATP	Fatty acid transporter protein
FID	Flame ionization detector
GC	Gas chromatography
HUFA	Highly unsaturated fatty acid
LA	Linoleic acid, 18:2n-6
LPL	Lipoprotein lipase
MESSI	Multiple simultaneous stable isotope
MG	Monoglycerides
MHC	Myosin heavy chain
MS	Mass spectrometry
MUFA	Monounsaturated fatty acid
NCI	Negative chemical ionization
NEFA	Nonesterified fatty acid
PCI	Positive chemical ionization
PFB	Pentafluorobenzyl
PL	Phospholipids
PUFA	Polyunsaturated fatty acid
SERCA	Sarco-endoplasmic reticulum Ca^{2+} ATPase
SFA	Saturated fatty acids
SIM	Selected ion monitoring
TG	Triacylglycerol
U-^{13}C	Uniformly labelled carbon-13

CHAPTER 1

INTRODUCTION

Polyunsaturated fatty acids (PUFA) are required for a wide range of physiological functions. The best characterized among them are the functions of eicosanoids that are enzymatically synthesized from PUFA and work as autocrine/paracrine hormones mediating a variety of functions such as immune response, blood pressure regulation, and blood coagulation (Samuelsson, 1983). Recent studies have uncovered further involvement of PUFA in fundamental cellular functions, including endocytosis/exocytosis (Schmidt et al., 1999), ion channel modulation (Leaf and Kang, 1996) and regulation of gene expression (Clarke and Jump, 1994). Although many studies have focused upon the liver as the primary site for PUFA metabolism in mammals, relatively little is known about other organs with respect to their uptake of PUFA or the manner in which these fatty acids are distributed to them. Thus, the recent studies on PUFA metabolism have shifted their attention away from liver towards other organs such as heart, kidney, liver, brain, testes and skeletal muscle (Bourre et al., 1990; Fu, Attar-Bashi, and Sinclair, 2001; Lin and Salem, Jr., 2007; DeMar, Jr. et al., 2008). The PUFA composition of skeletal muscle has been associated with various contractile properties (Ayre and Hulbert, 1996) and may play a role in improving obesity and insulin resistance (Kuda et al., 2009; Rossmeisl et al., 2009; Shimura et al., 1997). However, PUFA tracer studies in skeletal muscle (Lin and Salem, Jr., 2007; DeMar, Jr. et al., 2008) have provided us with fragmented information regarding muscle type differences in PUFA uptake and metabolism. The present thesis investigates how linoleate, linolenate and their major metabolites, are absorbed, distributed and retained in various muscle types (i.e. slow and fast twitch). To accomplish this purpose two

different approaches were followed; 1) a characterization in which the fatty acid compositions of the muscle types were systematically compared particularly with regard to their PUFA content, 2) a prospective approach through which the distribution of the isotopic labelled precursors and their major *in vivo* metabolites were followed among various muscle types after experimental animals were ingested with a single bolus of the labelled precursors.

BIOCHEMICAL AND PHYSIOLOGICAL FOUNDATIONS

1.1 Fatty Acids

1.1.1 Overview

Fatty acids are compounds synthesised in nature via condensation of a malonyl coenzyme A ($COOH\text{-}CH_2\text{-}CO\text{-}S\text{-}CoA$) unit by a fatty acid synthase complex. In general, fatty acids contain even numbers of carbon atoms in straight chains (only occasionally outside the range of C_{14} to C_{24}) with a carboxyl group at one extremity and with double bonds of *cis* (or Z) configuration. Based on the hydrocarbon chain length, fatty acids have been divided into four groups; short chain fatty acids ($\leq$ 6 carbons), medium chain fatty acids (8-12 carbons), long chain fatty acids (14-22 carbons), and very long chain fatty acids (>22 carbons). Fatty acids from animal tissues may have zero to six double bonds which are specified in systematic nomenclature in relation to the carboxyl group. Depending on the number of carbon-carbon double bonds, fatty acids are categorized as saturated (0), monounsaturated (1), and polyunsaturated (>1). The term HUFA (highly unsaturated fatty acids) has recently begun to be used in the literature to identify PUFAs with $\geq$3 double bonds and $\geq$ 20 carbons as this group of fatty acids have important structural and physiological roles (Nakamura et al., 2001).

1.1.2 Polyunsaturated fatty acids (PUFA)

PUFAs have two or more double bonds and are typically 18–22 carbon atoms long consisting of the omega-6 and omega-3 families of fatty acids, otherwise known as the n-6 and n-3 fatty acids. The n-6 and n-3 fatty acids differ from each other structurally by the position of their double bond from the methyl terminus (i.e. the "omega" end) at the 6th and the 3rd bond, respectively. They also differ functionally from each other and are not interconvertible, although they share and compete for several enzymes in their metabolic pathways (See **Figure 1**). Linoleic acid (LA; 18:2n-6) and alpha-linolenic acid (ALA; 18:3n-3) are considered as precursor fatty acids for the n-6 and n-3 families, respectively, as both LA and ALA can be further metabolized to HUFAs by the actions of delta-6 and delta-5 desaturases and elongase enzymes in tissues (Igarashi et al., 2007; Jump, 2002; Harris et al., 2008). These fatty acids each undergo three rounds of desaturation and three rounds of elongation, followed by β-oxidation to produce the final products 22:5n-6 and 22:6n-3 (Igarashi et al., 2007) (See **Figure 1**). LA and ALA are known as essential fatty acids in mammals as they cannot be synthesized *de novo* and they are required in the diet to prevent deficiencies (Pudelkewicz, Seufert, and Holman, 1968). In plants, algae and some bacteria, LA is synthesized by the action of delta-12 desaturase, which forms a double bond, six positions from the methyl end of 16- and 18-carbon monounsaturated fatty acids. This linoleic acid product can be further desaturated by delta-15 desaturase, which forms a double bond, three positions from the methyl end forming ALA (Morimoto et al., 2005). Important dietary sources of LA include vegetable oils such as corn oil, and those of ALA include green leaves and some oils such as flaxseed and canola oil (Burdge and Calder, 2005). Arachidonic aid (AA; 20:4n-6) and docosahexaenoic acid (DHA; 22:6n-3) are the major *in vivo* metabolic end products derived from LA and ALA, respectively. However the conversion

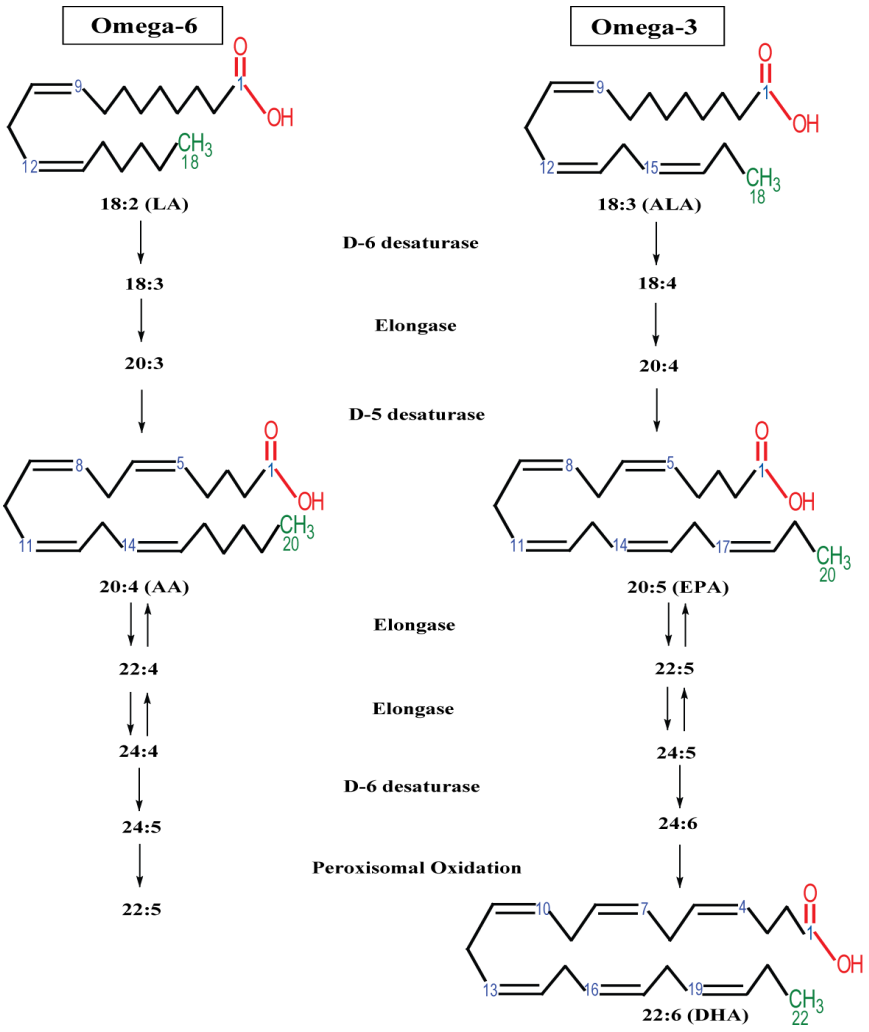

Figure 1. Polyunsaturated fatty acid biosynthetic pathway. LA: linoleic acid (18:2n-6); ALA: α-linolenic acid (18:3n-3); AA: arachidonic acid (20:4n-6); EPA: eicosapentaenoic acid (20:5n-3); DHA: docosahexaenoic acid (22:6n-3). Adapted from (Harris et al., 2008)

efficiencies of LA to AA, and ALA to DHA have been reported to be low with estimates of 1.4 % of dietary ALA and 3 % of dietary LA being converted to long-chain PUFAs in rats (Cunnane and Anderson, 1997b). AA is particularly important as the main component of membrane phosphoslipids, and as a precursor of the prostaglandins and other eicosanoid metabolites. DHA is particularly enriched in the phospholipids of cells constituting the mammalian nervous system

and consequently important for cognitive function and vision maturity and resolution (Carlson and Neuringer, 1999; SanGiovanni et al., 2000). Functionally, DHA enhances membrane elasticity and molecular motion and thus promotes signal transduction via enhanced protein/receptor interactions (Gawrisch, Eldho, and Holte, 2003). DHA can also serve as an activating ligand for multiple transcriptional factors that control the expression of enzymes involved in fatty acid synthesis and β-oxidation (Clarke and Jump, 1994). As one of the n-3 precursors for the eicosanoid production, DHA contributes to protection against inflammation and cardiovascular diseases (Calder, 2004).

1.1.3 Mechanism of fat digestion and absorption

The first step of fat digestion occurs in the stomach and is catalyzed by lingual or gastric lipase. The major digestion products of this gastric phase are diacylglycerol and nonesterified fatty acids (NEFA) (Thomson et al., 1989). Pancreatic lipase cleaves fatty acids at the *sn*-1 and *sn*-3 position of triacylglycerols yielding to 2-monoglycerides (2-MG) and NEFA (Carlier, Bernard, and Caselli, 1991). Dietary phospholipids are hydrolyzed by activated pancreatic phospholipase A2 yielding to 1-lysophospholipids and NEFA (Carlier, Bernard, and Caselli, 1991). The major products of lipid digestion, NEFA and 2-MG enter the enterocyte by simple diffusion across the plasma membrane. A considerable fraction of the fatty acids also enter the enterocyte via a specific fatty acid transporter protein in the membrane (Luiken et al., 2001). Absorbed lipids are re-esterified to form triacylglycerols (TG) and phospholipids (PL) in the smooth endoplasmic reticulum in the intestinal brush border. TGs, PLs, cholesterol and apoproteins are used to synthesize chylomicrons, which are secreted to the lymph and then to the general blood stream through the thoracic duct. In extra-hepatic tissues, the TG content of chylomicrons is hydrolysed in the capillaries by lipoprotein lipase attached to the outside of the

cells lining the blood capillaries to produce glycerol and NEFA which enter the adjacent cells. The amount of lipase activity present in the capillaries of a particular tissue determine the amount of NEFA release in that tissue and insulin can stimulate the lipase activity (Voet and Voet, 2004).

1.1.4 Effects of fatty acid chain length and saturation

Unsaturated fatty acids and medium chain fatty acids (MCFAs) are more efficiently absorbed than long-chain saturated fatty acids. Because of the way that MCFA are digested, they can be absorbed in the stomach, after hydrolysis of medium chain TG by gastric lipase (Christensen et al., 1995), and can also be solubilized in the aqueous phase of the intestinal contents, where they are absorbed bound to albumin and transported to the liver via the portal vein (Decker, 1996). With increasing chain lengths of saturated fatty acids, an increasing proportion is absorbed into the lymphatic pathway and a decreasing proportion is absorbed by way of the portal venous blood (Thomson et al., 1989).

1.1.5 Fat oxidation

The first stage in oxidation of fatty acids is to convert the NEFA to a fatty acyl-CoA compound, a reaction known as fatty acid activation. Activated fatty acids are subsequently broken down by removing two carbon atoms at a time as acetyl-CoA, a process known as β-oxidation. Activation of fatty acids occurs in the outer mitochondrial membrane but their conversion to acetyl-CoA occurs only in the mitochondrial matrix. The acyl group of fatty acyl-CoA is carried through the inner mitochondrial membrane, without the CoA, by a special transport mechanism (i.e. carnitine cycle) then handed over to CoASH in the mitochondrial matrix to become fatty acyl-CoA again. Long-chain fatty acids (LCFA) which encompass

PUFAs enter the mitochondrial space via the carnitine cycle, whereas short- and medium-chain fatty acids enter directly in their protonated form (Christie, 1989) (See **Figure 2**).

1.1.6 β-oxidation

The reaction sequence in each round of the β-oxidation involves conversion of β carbon atom (i.e. the third carbon from carboxyl end) to a C=O group, forming a β-ketoacyl-CoA through reduction, oxidation and reduction reactions. The ketoacyl-CoA is cleaved by CoASH, splitting off two carbon atoms as acetyl-CoA and forming a shorter fatty acyl-CoA derivative. Oxidation of unsaturated fatty acids requires an isomerase reaction to position existing double bonds on the normal metabolic path of β-oxidation (Christie, 1989).

1.1.7 Peroxisomal oxidation

In animal cells, mitochondria and peroxisomes oxidize fatty acids via β-oxidation. The major differences between peroxisomal and mitochondrial β-oxidation include; different substrate specificities, transport of substrates and products of β-oxidation across the membrane. Short and medium-chain fatty acids are exclusively, and long-chain fatty acids are predominantly oxidized in mitochondria, whereas very long-chain fatty acids, notably 26:0, can only be handled by peroxisomes. Peroxisomal oxidation of fatty acids does not generate ATP (Wanders and Waterham, 2006).

1.2 Skeletal Muscle and Fatty Acids

1.2.1 Skeletal muscle diversity

One of the unique features of skeletal muscle is its composition of a large number of different types of muscle fibres which contribute to a variety of functional capabilities present in

skeletal muscle. These fibre types can differ and be categorized according to their molecular, metabolic, structural and contractile properties. The diversity of the skeletal muscle was recognized as early as 1873 when Ranvier categorized red muscles with slow contraction and white muscles with fast muscle contraction based upon appearance and stimulation of the muscle with electrical current (Ranvier, 1873). Various fibre type classification schemes were developed but only a few are widely used. To date, the most useful schemes to delineate fibre types are based on histochemical and electrophoretic differences in myosin ATPase activity of myosin heavy chain (MHC) isoforms (Staron and Pette, 1986). According to the major MHC isoforms found in the adult mammalian skeletal muscles, the following pure fibre types can be delineated; slow type I with MHCIβ, slow cardiac MHC isoform, and three fast types, namely type IIA with MHC isoform IIa, type IID with MHCIId, and type IIB with MHCIIb, while MHCIId and fibre type IID are considered to be equivalent to MHCIIx and fibre type IIX, respectively (Pette and Staron, 1990; Schiaffino and Reggiani, 1994). Both nomenclatures, therefore, coexist in the literature. Comparative studies on various mammals have revealed that as body mass increases, expression levels of the slower MHC isoforms increase at the expense of faster isoforms (Aigner et al., 1993; Hamalainen and Pette, 1995). For instance, it was shown that type IIB fibres comprise 71% of the total mass of the muscle in rats followed by type IID/X 18% , type IIA 5% and type I 6% (Delp and Duan, 1996), while muscle in human and other large mammals do not appear to express MHCIIb. Fibres previously classified as type IIB in human muscle have therefore been renamed type IIX or type IID, based on their MHC complement that resembles MHCIIx (MHCIId) of the rat. Some of the most important functional and morphological properties of the MHC-based fibre types are summarized in **Table 1**. It has been shown that the

oxidative potential of rat muscle is greatest when composed of type IIA fibres and in the rank order of type IIA > I > IID/X > IIB fibres (Delp and Duan, 1996).

Table 1. Common classification of skeletal muscle fibre types and fibre type percentages in the same muscle across different species

	Classification scheme			
Contractile speed	Slow-twitch	Fast-twitch	Fast-twitch	Fast-twitch
Myosin heavy chain	Type I	Type IIA	Type IIX/D	Type IIB
Metabolic	Oxidative	Oxidative-glycolytic	Glycolytic	Glycolytic
Anatomical (color)	Red	Red	White	White
Fibre CSA	Small	Medium	Large	Large
	Average % in V. Lateralis			
Human[1]	40	30	30	n/d
Rat[2]	1	36	n/d	63
Mouse[3]	0	30	n/d	70

[1]Humans do not typically express IIB myosin heavy chain in the locomotor skeletal muscles (Andersen, Schjerling, and Saltin, 2000; Smerdu et al., 1994). [2]Rat (Armstrong and Phelps, 1984) and [3]mouse (Burkholder et al., 1994) did not delineate the fast fibre types into IIX and IIB subtypes, therefore IIX and IIB subtypes are likely combined in the IIX fibre data. CSA, cross sectional area; n/d, not detected. Adapted from (Spangenburg and Booth, 2003).

1.2.2 Fat transport across muscle membrane

Movement of fatty acids from the interstitium across the plasma membrane differs for short and medium chain fatty acids, relative to long and very long chain fatty acids. Transport of short and medium chain fatty acid into muscle and across mitochondrial membranes is fully dependent on passive diffusion dictated by the concentration or driving gradient of these fatty acids. This phenomenon is known as “flip-flop” and involves a number of discrete and sequential steps including; movement of fatty acids to the outer leaflet of the phospholipid bilayers, insertion into the outer phospholipid bilayers, flip-flop across the membrane, dissociation from the inner phospholipid bilayers, and rendering the fatty acid inside the cell or mitochondrial

matrix (Noy, Donnelly, and Zakim, 1986). For LCFA which encompass all PUFAs, fatty acid transport into muscle and subsequently into mitochondrial matrix occurs largely through a highly regulated protein-mediated mechanism involving a number of fatty acid transporters. Three types of transport proteins have been identified; a fatty acid binding protein (FABPpm) located on the outer leaflet of the plasma membrane, a family of fatty acid transport proteins (FATP1–6) that have at least six transmembrane domains, and a highly glycosolated fatty acid translocase (FAT/CD36) (FAT is the homologue of human CD36) that has at least 2 transmembrane domains (Abumrad, Coburn, and Ibrahimi, 1999). FABPpm and FAT/CD36 are expressed in proportion to the rate of LCFA oxidation in muscle tissues (heart >> red muscle >> white muscle) (Bonen et al., 1998; Chabowski et al., 2006). Studies using confocal immunofluorescence microscopy (Keizer et al., 2004) have shown that FAT/CD36 and FABPpm are harboured at the level of the plasma membrane and in an intracellular depot. Similar to the glucose uptake by skeletal muscle, LCFA transport can also be regulated within minutes by muscle contraction, AMP-activated protein kinase activation, leptin, and insulin (Nickerson et al., 2007) through the induction of the translocation of FAT/CD36 (Bonen et al., 2000; Chabowski et al., 2005) and FABPpm (Chabowski et al., 2005; Han et al., 2007) from their intracellular depot to the plasma membrane. It has been hypothesized that in insulin-resistant muscle, a permanent relocation of FAT/CD36 to the sarcolemma may account for the excess accretion of intracellular lipids that interfere with insulin signalling. Inside the cell, LCFA remain water insoluble and are bound to FABPc or acyl-CoA binding protein. It has been suggested that FABPc likely works in a concerted fashion with FAT/CD36 to transport LCFA across the plasma membrane (Luiken et al., 1999). A schematic diagram of fatty acid

transportation across sarcolemma into muscle and subsequently into mitochondria is presented in **Figure 2**.

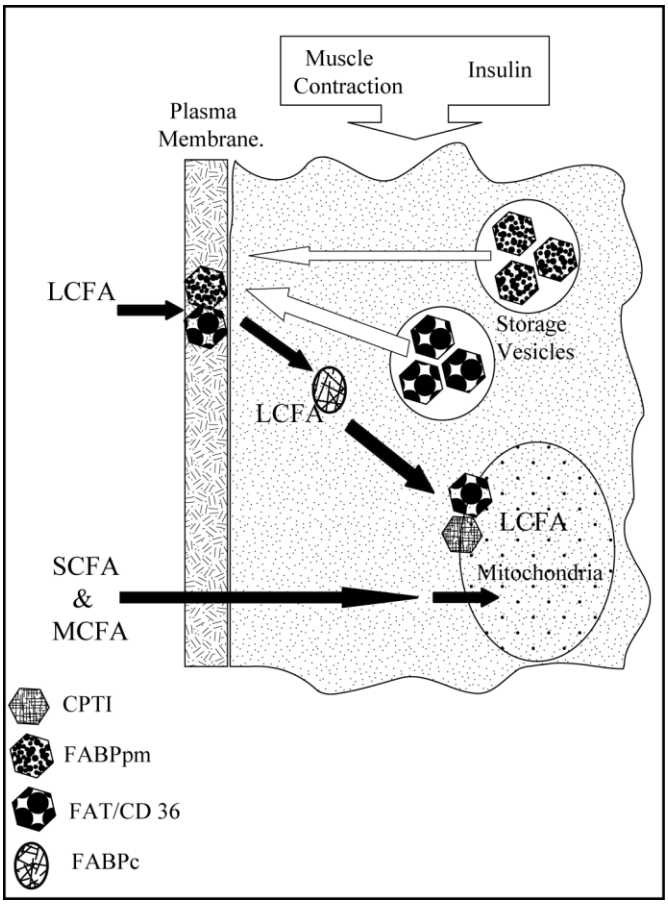

Figure 2. Fatty acid uptake in skeletal muscle and oxidation in mitochondria. LCFA: long chain fatty acid; SCFA: short chain fatty acid; MCFA: medium chain fatty acid; CPTI: Carnitine palmitoyl transferases I; FABPpm: Fatty acid binding protein pm; FAT: fatty acid translocator; FABPc: Fatty acid binding protein c. Adapted from (Holloway et al., 2008).

1.2.3 Fat metabolism in skeletal muscle

Fatty acids originating from chylomicrons and very-low-density lipoproteins are hydrolyzed by lipoprotein lipase (LPL) and subsequently are taken up by muscle, esterified in the sacroplasmic reticulum to triacylglycerol, and incorporated into lipid droplets in muscle (**Figure 3**). It has been shown that in the postprandial state there is a clear preferential uptake of fatty acids derived from LPL-mediated chylomicron hydrolysis into skeletal muscle as compared with plasma NEFAs or very-low density lipoprotein derived fatty acids (Bickerton et al., 2007;

Evans et al., 2002). This suggests higher absorption of dietary fatty acid or those ingested compared to those being delivered intravenously. Most fatty acids entering muscle cells from circulation are rapidly esterified to TGs (70-90%), with the remaining fatty acids being maintained in a NEFA pool. During muscle contraction, fatty acids are predominantly derived from the adipose tissue and intramuscular TG (Kiens, Roemen, and van der Vusse, 1999). Lipolysis in adipose tissue and in intramuscular TG is regulated by a hormone sensitive lipase (HSL) which is activated by beta-adrenergic receptors (Coyle, 1999). It appears that the two lipases (i.e. LPL and HSL) function as a coordinated unit in meeting the energy demands of muscle. Both LPL and HSL are regulated, in part, through the classic cAMP cascade in muscle. However, the functions of these lipases are different. While activation of HSL results in the hydrolysis of intracellular TG, providing fatty acids for β oxidation, the exported LPL found in the capillary beds hydrolyzes circulating TG, providing fatty acids for the replenishment of lipid stores and, to a lesser extent, immediate substrate for muscle energy needs. The activities of LPL and HSL are the highest in the soleus, lower in the red portion of gastrocnemius, and undetectable in the white portion of gastrocnemius (Smol et al., 2001). However, removing the normally high level of postural support by red oxidative muscles (i.e. Type I and Type IIA) can abolish up to 95% of LPL activity differences between muscle fibre types (Oscai, Essig, and Palmer, 1990). This suggests that the difference in LPL activity between fibre types is primarily due to the level of recruitment in normal daily activity rather than intrinsic factors such as cellular lineage or neurotrophic factors.

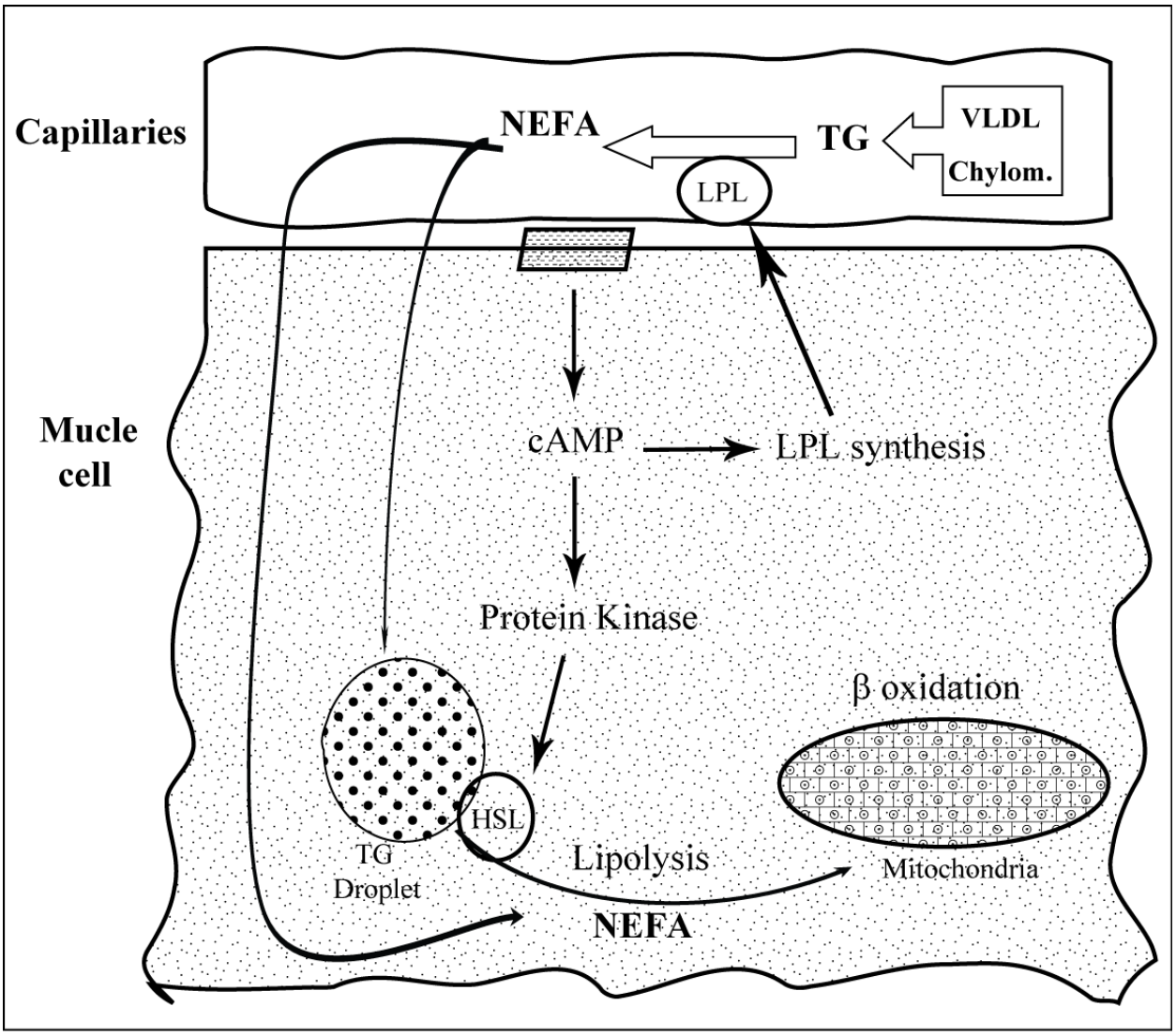

Figure 3. Muscle fatty acid metabolism and proposed mechanism for regulation of hormone-sensitive lipase (HSL) and lipoprotein lipase (LPL). VLDL; very low density lipoprotein, Chylom; chylomicron, TG; triacylglycerols, NEFA; nonesterified fatty acids, cAMP; cyclic adenosine monophosphate.

1.2.4 Effect of PUFA on muscle function

A number of studies have shown that a high-fat diet can dramatically increase exercise performance in rats (Miller, Bryce, and Conlee, 1984; Simi et al., 1991) and humans (Lambert et al., 1994; Muoio et al., 1994). However exercise (resistance or endurance) is a multifactorial

phenomenon in which the observed effects of dietary changes may reflect changes in the respiratory and/or cardiovascular systems rather than on the muscles themselves. Therefore, study designs with higher level of specificity are required to elucidate the role of PUFAs on muscle function. The effects of manipulating dietary levels of essential PUFAs on several aspects of muscle function (i.e. single muscle twitch, sustained tetanic contractions, posttetanic potentiation, sustained high-frequency stimulation, and intermittent low-frequency stimulation) were examined in rats using *in vitro* preparations of extensor digitorum longus (EDL; fast twitch) and soleus (slow twitch) muscles (Ayre and Hulbert, 1996). Rats fed a PUFA-deficient diet relative to PUFA enriched diets had significantly lower muscular tensions and reduced response times with twitch contraction and half relaxation times significantly reduced by 5-7%. Also, with the PUFA-deficient diet, peak twitch tension in soleus muscles was 16-21% less and EDL muscles fatigued 32% more quickly. These differences disappeared once PUFAs were added to the deficient diet and the pattern of recovery of muscle performance mirrored the pattern of changes in the muscle phospholipid composition.

Because phospholipids are the major structural lipid in membranes, changes in the dietary fatty acid profile could also have profound effects on membrane physical properties. For example, essential PUFAs deficiency may affect the fluidity of membranes (McMurchie, 1988) and therefore possibly exert influence over specific membrane proteins, such as enzymes (Murphy, 1990), or have a controlling influence on transport of small molecules across cell membranes (Sahlin et al., 1981). Consistent with these observations, 3 wks of supplementation with high PUFA diet significantly increased the activity of Na^+,K^+ ATPase enzymes in isolated soleus muscles (Early and Spielman, 1995). Furthermore, phosphatidylserine and phosphatidylglycerol, two phospholipids generally high in PUFAs, have shown to stimulate this

enzyme to a greater extent than do phosphatidylinositol, phosphatidylethanolamine, phosphatidylcholine or diphosphatidylglycerol (Wheeler, Walker, and Barker, 1975). Consequently these changes in Na^+,K^+ATPase activity in response to changes in phospholipid content may more reflect changes in the PUFA content of the membrane.

In a retrospective study, the fatty acid composition of high-frequency contraction muscles in hummingbirds (i.e. pectoral muscles) and rattlesnakes (i.e. shaker muscles) were compared with other muscles in the same species known to have much lower contraction frequency (i.e. leg muscles and ventral muscles, respectively) (Infante, Kirwan, and Brenna, 2001). The concentration of 22:6n-3 was 20.8% in hummingbird pectoral muscles versus 4.9% for the low contraction frequency leg muscles and 15.1% in rattler muscles in rattlesnakes versus 10.6% for lower contraction frequency ventral muscles. The dramatic differences in the 22:6n-3 concentrations between high and low frequency contraction muscles in the same species suggest that in high-frequency contraction muscles, 22:6n-3 enriched phospholipids are required to support the optimal functioning of ion pump activity of sarcoplasmic reticulum Ca^{2+}-ATPase (SERCA) and electron transport in the mitochondria (Infante, Kirwan, and Brenna, 2001). In both, sarcoplasmic reticulum and mitochondria, PLs consist of approximately 80% of total lipids with TG being the dominant neutral lipid and both fractions have similarly high percentages of 22:6n-3(approximately 20%) (Fiehn et al., 1971). The 22:6n-3-containing PL species are the most abundant PL species in rat sarcoplasmic reticulum (Fiehn et al., 1971) and the fact that SERCA represents approximately 90% of the total sarcoplasmic reticulum protein in fully differentiated skeletal muscle (MacLennan and Holland, 1975; Fiehn et al., 1971) further strengthens the correlation between 22:6n-3 content and SERCA function.

1.2.5 Muscle structural lipids and fatty acids

Membrane PLs are the major structural lipids accounting for approximately 75% of total lipids in the skeletal muscle (Blackard et al., 1997). All six PL species presented in the skeletal muscle are listed here in the order of their abundance in the skeletal muscle; phosphatidylcholine, phosphatidylethanolamine, cardiolipin, sphingomyelin, phosphatidylserine, and phosphatidylinositol (see **Figure 4** for chemical structures). Phosphatidylcholine and phosphatidylethanolamine make up over 70% of the total PLs. These PL species serve as the main reserve of PUFAs, either for the short-time regeneration of PUFAs that have been degraded during membrane stimulation or for substrates for a variety of signalling molecules. It is difficult to use dietary manipulation to alter the ratio of saturated to unsaturated fatty acids in membrane PLs because of the biochemical preference for a saturated fatty acid in the *sn*-1 position and an unsaturated fatty acid in the *sn*-2 position in PLs (Stubbs and Smith, 1984). This homeostatic mechanism may therefore maintain a relatively constant level of membrane fluidity despite large fluctuations in dietary fatty acid profile. Although it is not possible to greatly alter the ratio of saturated to unsaturated fatty acids in muscle PLs, it is possible to change the proportions of the different classes of unsaturated fatty acids. The greatest difference in PL fatty acid content between type I and type IIB muscle fibres was reported in the saturated fatty acids of the phosphatidylcholine species (Blackard et al., 1997). EDL muscle, constituting of 58% type IIB fibre in rat (Delp and Duan, 1996) had a much higher 16:0 and a significantly lower 18:0 compared to soleus muscle. 18:2n-6 and 18:3n-3 fatty acids tend to be similar in the phosphatidylcholine fractions between these muscle types. Longer-chain n-3 fatty acids (22:5n-3 and 22:6n-3) have been reported to be decreased in phosphatidylcholine from EDL as compared with soleus, but long-chain n-6 fatty acids such as 20:4n-6 did not differ (Blackard et al., 1997).

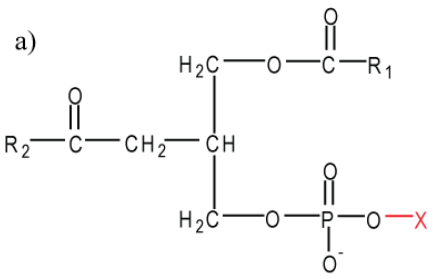

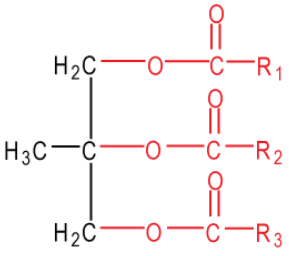

Name of X - OH	Formula of - X	Name of Phospholipid
Ethanolamine	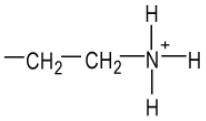	**Phosphatidylethanolamine**
Choline	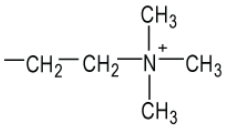	**Phosphatidylcholine (Lecithin)**
Serine	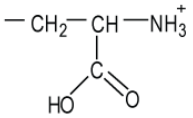	**Phosphatidylserine**
Phosphatidylglycerol	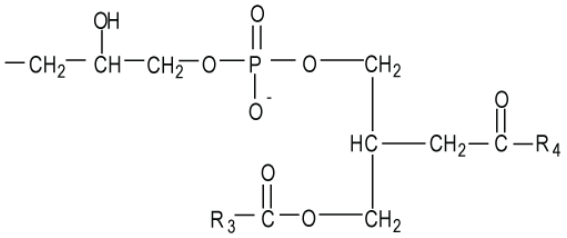	**Diphosphatidylglycerol (Cardiolipin)**
Myo-Inositol	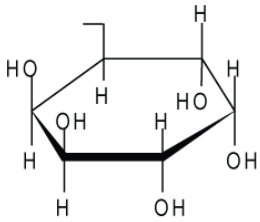	**Phosphatidylinositol**

Figure 4. The common classes of phospholipids. a) Molecular structure of a typical phospholipid b) Molecular structure of a typical triglycerol moiety. R1, R2 and R3 indicate sn-1, sn-2 and sn-3 positions, respectively and they are schematic representation of the hydrocarbon chain of a fatty acid.

CHAPTER 2

METHODOLOGICAL FOUNDATIONS

2.1 Fatty Acid Stable Isotope Measures by Gas Chromatography Mass Spectrometry

2.1.1 Gas chromatography (GC)

The process of chromatography involves partition of the components of a mixture between two phases, a mobile phase and a stationary phase. The technique of gas-liquid chromatography or gas chromatography is a form of partition chromatography in which the mobile phase is a gas and the stationary phase is a liquid. A basic gas chromatograph has three essential components; an injector, the column, and a detector. Fatty acid methyl esters (FAME), dissolved in a non-polar solvent such as hexane, are first vaporized in the injection port at temperatures nearing 300ºC. A carrier gas such as hydrogen or helium then carries the gaseous fatty acids to the column as the mobile phase. The inside of the column is coated with a liquid compound that is the stationary phase. In order to speed the movement of the gaseous fatty acids through the column, it is necessary to raise the column oven temperature in a systematic fashion up to temperatures nearing 250ºC. As the gaseous fatty acids move through the column, they interact with the stationary phase. Factors relating to the chemical makeup of the stationary phase, for example its polarity, as well as the molecular weight and structure of the fatty acids determine the delay between the injection of the sample and each fatty acids column exit, also termed “retention time” (Christie, 1989). The longest chain and most unsaturated fatty acids have the longest retention times. Separations using conventional GC techniques typically lasted up to 120 minutes. Advances in GC techniques have allowed this time to be reduced to as low as 8

minutes (Masood, Stark, and Salem, Jr., 2005). Upon exiting the column, the sample is analyzed by a detector. For fatty acids, a flame ionization detector (FID) is commonly used, which uses a hydrogen flame to combust the hydrocarbon chain. This combustion produces ions, which contact an electrode, resulting in a measurable electronic current that is converted into a response curve or "peak" for each fatty acid. The area under the curve for each peak can be integrated to quantify the fatty acids. The advantages of the FID include simple design, low cost and low maintenance, high sensitivity, and linear responses (Christie, 1989). A standalone GC can be used to analyze individual fatty acids from a total lipid extract. The GC can also be coupled to a MS with the MS serving as the detector.

2.1.2 Mass Spectrometry (MS)

The key components of a mass spectrometer are the ion source, the mass analyzer and the detector. The principle of the technique in its simplest form is that organic molecules in a vapour phase are bombarded with electrons and form positively charged ions. These ions are analyzed by the means of mass analyzer based on their mass to charge ratio (m/z). Subsequently they are collected and detected in sequence as the ratio increases with an amplified signal of each (m/z) ratio recorded and visualized by a computer. Of the many different ionization techniques in use today, electron ionization (EI) and chemical ionization (CI) are the most common in the field of lipid research. Both have unique advantages and certain key limitations (**Table 2**).

In EI, electrons are first produced by heating and passing a current through a thin filament. The collision of electrons with the sample molecules (M), leads to their ionization by electron loss with the formation of the molecular ion $M^{+\bullet}$. CI is related to the EI method except that ionization of a reagent gas (e.g. methane or isobutane), rather than the sample molecule itself, occurs first. This is followed by the transfer of charge to the sample molecule by a

chemical process. The indirect ionization via a CI method is a much softer ionization technique relative to EI and can greatly reduce fragmentation of the sample analyte, resulting in a higher proportion of unfragmented analyte or "parent ion". Many different reagent systems have been used to significantly improve sensitivity and resolution of CI-MS. The choice of reagent system depends on analytical requirements such as sensitivity, resolution, and linear quantitation (Barker, 2000). Chemical ionization reagents include methane, hydrogen gas, isobutane, methanol, and ammonia. Two CI methods have been developed; positive chemical ionization and negative chemical ionization.

Table 2. Advantages & disadvantages of EI vs. CI

	EI		**CI**
	Hard Ionization		Soft Ionization
Cons	High levels of fragmentation	**Pros**	Low levels of fragmentation
	Low level of parent ion		High levels of parent ion
	Low quantitative values		High quantitative values
	Single method of ionization		Multiple choice of reagent ions
	Consistent spectra		Incongruent spectra
Pros	EI mass spectra library	**Cons**	No CI mass spectra library
	High qualitative values		Moderate qualitative values
	Low maintenance		High maintenance

2.1.3 Positive chemical ionization (PCI)

Chemical ionization using positively charged reagent ions is termed positive chemical ionization. Lower sample fragmentation and higher selectivity in sample ionization contribute to the higher sensitivity and resolution of PCI as compared with EI. The low internal energy associated with the PCI protonation process results in a much lower excitation state for the ionized sample molecule. As a result, fragmentation in PCI is lower than EI (Harrison, 1992).

The efficiency of the protonation process depends in part on the sample's proton affinity and the reagent's acidity, both of which can be manipulated. Thus it is possible, through certain sample preparation techniques, to increase the proton affinity of a desired set of compounds in complex mixture so as to ensure that only those particular compounds are ionized by reagent ions (Harrison, 1992).

Fragmentation in PCI takes place through several complex processes that lead to the formation of certain distinct types of fragments. These fragments can be monitored to enhance the sensitivity of detection and accuracy of quantification. The most common of these fragmenting processes include small mass fragmentation, high mass fragmentation, hydride abstraction, and adduct formation (Berberich et al., 1989).

2.1.4 Negative chemical ionization (NCI)

In negative CI, energetic electrons are first reacted with a reagent gas. This reaction causes the electrons to impart much of their energy onto the reagent molecules, and in the process become low energy or "thermal" electrons. These thermal electrons can then readily attach to molecules with high electron affinity (Harrison, 1992). This technique is also known as "electron-capture" chemical ionization. Since this electron capture occurs with very little internal energy, there is even less fragmentation of the sample molecule as compared with PCI (Harrison, 1992). As well, sample preparation techniques allow for the ionization of very select groups of compounds, significantly reducing background ionization. These two factors give NCI higher sensitivity and resolution as compared with PCI (Harrison, 1992). Limits of detection for fatty acids have been reported at as low as 20fg/uL (Goto et al., 1987), and responses more than 2000 times higher than PCI (Pawlosky, Sprecher, and Salem, Jr., 1992). Less fragmentation also means more available sample, and therefore lower sample concentration requirements (Harrison,

1992). However, NCI is not without its limitations. These include complex and time-consuming sample preparation techniques, and high equipment maintenance demands. Fatty acid analysis with NCI requires preparation of pentafluorobenzyl (PFB) esters. The PFB group enables the fatty acid to be more electrophilic so as to better attract thermalized electrons. The entire PFB derivitization process requires more steps than methyl ester formation that is done in PCI. It also requires larger volumes of solvents such as hexane, and longer dry times under N_2. The electron capture process also requires the availability of a larger volume of thermal electrons. As a result, the filament emission current in NCI is more than 15 times higher than that of PCI. This results in shorter filament operating times which is not trivial as filament assemblies are expensive, and instrument shutdown results in significant post start-up diagnostics and tuning.

2.1.5 Mass-selection

Mass-selection allows for the selection of a single reagent ion, based on its mass, and then allows only that selected reagent ion to ionize the sample. Using this technique, the reagent ion with the lowest energy can be used thereby minimizing the fragmentation of the parent compound. Mass-selection techniques have been demonstrated in environmental contaminant assessments for PCBs (Lausevic et al., 1995), and alkylbenzenes (Berberich et al., 1989) but not for fatty acid analysis. Mass-selection was used in the development of the novel internal isobutane technique for this thesis. Detailed scanning procedures for mass-selection are provided in Methods under “Mass selection”.

2.1.6 Selected ion monitoring

Selected ion monitoring (SIM) generates peaks that correspond to the abundance of one or more user-defined ion masses. This tool was used in all isotopic quantification work in this

thesis. Fatty acid stable isotopes labelled with ^{13}C co-elute chromatographically with endogenous unlabelled fatty acids. As a result, the total ion chromatographic peak cannot be integrated to quantify the isotope. The first step is to select for the most abundant ion of a FAME, by its mass to charge (m/z) value. In PCI however, any given FAME generally produces more than one high mass fragment ions. **Table 3** below lists some of the common ion m/z values that are used in SIM to quantify the respective isotopic FAMEs. When more than one m/z is used in SIM, the response is amplified, the shape of the chromatographic peak is clearer, and is thus simpler to quantify.

Table 3. Mass to charge (m/z) values of select isotopic FAMEs, ionized using isobutane PCI.

Isotopic FAME	Monitored m/z values
$^{13}C_{18}$-18:2n-6	**313**, 311, 281
$^{13}C_{18}$-20:3n-6	**339**, 337, 307
$^{13}C_{18}$-20:4n-6	**337**, 335, 305
$^{2}H_{5}$-18:2n-6	**284**, 282, 252
$^{2}H_{5}$-20:3n-6	**310**, 308, 278
$^{2}H_{5}$-20:4n-6	**308**, 306, 276
$^{2}H_{5}$-18:3n-3	**298**, 266
$^{2}H_{5}$-20:5n-3	**322**, 290, 272, 244, 220
$^{2}H_{5}$-22:6n-3	**348**, 316, 298, 288, 274
$^{13}C_{16}$-16:0	**287**
$^{2}H_{2}$-18:1n-9	**299**

Bolded numbers are parent ion m/z values; the rest are other high-mass fragment ions. FAME, fatty acid methyl esters; PCI, positive chemical ionization; m/z, mass to charge ratio.

2.1.7 Feasibility of present MS techniques

Presently, GC-MS techniques used for fatty acid stable isotope analyses include transmission quadrupole, isotope ratio mass spectrometry (IRMS), and quadrupole ion trap.

Each type of GC-MS technique has unique properties particularly in regards to the ionization of the analyte and separation of the ions before detection.

Transmission quadrupole mass spectrometer consists of four precisely straight and parallel rods arranged that the beam of ions from the ionization source of the spectrometer is directed axially between them. Direct current and radio frequency currents are applied between adjacent rods, opposite rods being electrically connected. As these voltages are increased, ions with increasing instability are ejected from the tunnel and propelled toward the detector (Barker, 2000). The resolution of the spectrometer can be increased by either employing eight poles or by connecting two or three quadrupoles in series.

In IRMS, samples are generally combusted or pyrolyzed completely and the desired elemental species is then detected. For an isotopic sample containing ^{13}C, the compound is combusted to CO_2 gas, ionized and propelled to the detector. The process is element-specific and therefore must be changed to allow analysis of isotopic N, O, S, etc. (Godin, Fay, and Hopfgartner, 2007). This allows for greater sensitivity and accuracy in determining specific isotope ratios. However, it is critical that analytes are completely separated before entering the mass spectrometer, so only one compound at a time is analyzed. IRMS requires cleaner and higher sample concentrations, is more expensive, and requires dedicated and highly trained technical personnel (Godin, Fay, and Hopfgartner, 2007).

An ion trap assembly consists of three electrodes; a ring electrode, an entrance electrode, and an exit electrode that are separated by quartz spacers and contained in a heated oven. These electrodes have hyperbolic inner surfaces that together form a cavity in which ionization, fragmentation, storage, and mass analysis take place. This allows ionization to take place at low pressures, and with extremely low sample concentrations. It is also possible to selectively eject

desired ions to the detector which enables MS^n analyses. These factors combined with the very short distance between the trap and the detector allow for very high sensitivity and resolution compared to transmission quadrupole analyzers where ions flow continuously from the ionization source to the detector (Barker, 2000; Downward, 2004). The ion trap MS is also fairly resilient instrument that is less technically demanding than an IRMS.

The Varian 4000 quadrupole ion trap GC-MS is capable of operating in three distinct ionization configurations; internal, external and hybrid. When the system is in internal configuration, analytes eluting from GC column directly enter the trap and ions are generated in the ion trap via electrodes that resides just outside the trap's entrance electrode. In external configuration, after the sample is ionized outside the trap in an external source, three lenses are used to direct the resulting ions towards the trap using electrostatic focusing. Hybrid configuration is a new ionization technique for quadrupole ion trap GC-MS systems which combines the valuable features of external ionization and internal ionization with removal of the critical issues for both. In the hybrid configuration reagent ions are generated in the external source and then drawn into the trap and only those selected are allowed to react with analytes eluting from GC column directly inside trap. This approach has a number of potential advantages including; avoiding ion molecules reactions with the neutral reagent and avoiding losses of sample ions that occur when they move from external source to the trap (Varian, 2006).

2.2 Fatty Acid Stable Isotope Tracer Study in Skeletal Muscle

2.2.1 Study design options

The single-labelled experimental design is the most widely used approach in tracer studies and involves administration of a pulse (i.e. one-time dosing) oral bolus of one labelled

fatty acid. A superior approach is the multiple simultaneous stable isotope design (MESSI) that involves administration of a pulse oral bolus of a mixture containing two or more labelled fatty acids (Emken, 2001). The advantage of the latter design compared to the former is that the metabolic fate of two or more fatty acids can be directly compared in the same subject under identical experimental conditions. Other advantages of the MESSI design are that a labelled fatty acid, such as oleic acid (18:1n-9), can be used as an internal standard and each subject can serve as his or her own control. As an example of the latter design, fractional synthesis rates of intramuscular TG in rat gastronemius and soleus muscles were evaluated using two isotopic labelled fatty acids (i.e. U-^{13}C palmitate and 1-^{13}C oleate) and it was found that the fractional synthesis rates of intramuscular TGs in gastrocnemius were significantly higher as compared with soleus for palmitate ($P = 0.04$) and oleate ($P = 0.02$) (Guo and Jensen, 1998).

Gavage is the method of choice for the oral administration of stable isotope fatty acids due to the consistency in delivering an accurate dose of stable isotope into the digestive tract of the experimental animals. With gavage, the desired food or nutrients are generally delivered to the stomach by passing a feeding tube or a blunt needle through the nose or mouth into the esophagus. Besides its application in research, gavage has been used frequently in medicine particularly to feed babies who are not able to suck or swallow enough of good nutrition.

2.2.2 Stable isotope options

Deuterated (^{2}H) and carbon 13 (^{13}C) labelled fatty acids are the most widely used stable isotope fatty acids in human and animal studies (Burdge and Wootton, 2002; Lin and Salem, Jr., 2007; DeMar, Jr. et al., 2008). ^{13}C isotopes have a smaller mass difference and similar physiological properties to ^{12}C, but endogenous fatty acids can suppress ^{13}C signals more than deuterated signals in a mass spectrometer (Lin, Pawlosky, and Salem, Jr., 2005). The deuterated

isotopes (typically D-5 at the two terminal methyl end carbons) are useful in tracking the fate of the original fatty acid while the uniform labelling of ^{13}C (U-^{13}C) isotopes provides the ability to potentially track the metabolic fate of the labelled fatty acid including oxidation to CO_2 if gas analyzers are utilized (McCloy et al., 2004). The typical amount of tracer in a pulse-oral-dose *in vivo* experiment is 30-50 mg/kg body weight of 95% enriched deuterated labelled fatty acid as compared with 2-10 mg/kg body weight of a 99% enriched U-^{13}C labelled fatty acids (Emken, 2001).

2.2.3 Issues

Delivering a consistent dose of isotopically labelled fatty acids to all of the experimental animals is the major issue due to the micro scale of the dose and the viscous nature of the fatty acids. In addition, expression of the isotope data can be challenging. Stable isotope tracer data has been expressed in a variety of units (e.g. percentage enrichment, tracer/tracee ratio, weight, and percentage of total tracer). In addition advanced modelling is also often used. Each approach has advantages and disadvantages, but presently there is no standard method of expression.

CHAPTER 3

RATIONALE & OBJECTIVES

3.1 RATIONALE

Previous investigations using stable isotope method have provided detailed analysis of PUFA uptake and metabolism by the liver, nervous system and blood (Sheaff et al., 1995), and some examination of other organs such as heart, lung and kidney (Su et al., 1999). Nevertheless the number of studies dedicated to the analysis of PUFA uptake and metabolism in skeletal muscle are limited and their findings are trivial with respect to the fibre type differences (DeMar, Jr. et al., 2008; Lin and Salem, Jr., 2007). Consistent and striking discrepancies in the PUFA content between different muscle types addressed in numerous compositional studies (Gorski, Nawrocki, and Murthy, 1998; Infante, Kirwan, and Brenna, 2001; Stark, Lim, and Salem, Jr., 2007) imply fibre type discrimination in PUFA uptake and metabolism. Moreover, the PUFA requirements may differ between muscle types possibly due to fibre type-specific SERCA activity and mitochondrial oxidation function. To our knowledge, this study will be the first work to offer comprehensive results on the uptake, distribution, and incorporation of PUFA stable isotopes in specific muscle types (i.e. soleus, red and white gastrocnemius). The anticipated results from these studies would lead to a much greater understanding of the role of fatty acids, particularly PUFA, in skeletal muscle function and would be the first step toward understanding of PUFA requirements for the optimal muscle function within specific fibre types.

3.2 OBJECTIVES

The overall objective of this thesis is to compare PUFA distribution and metabolism in skeletal muscle types with distinct fibre type composition; namely soleus (slow-twitch oxidative), red gastrocnemius (fast-twitch oxidative), and white gastrocnemius (fast-twitch glycolytic) up to 48 h. The first objective is to quantify the endogenous pools of fatty acids in the muscle types to confirm previously published results of PUFA differences between various muscle types (Blackard et al., 1997; Gorski, Nawrocki, and Murthy, 1998; Kriketos et al., 1995; Nikolaidis, Petridou, and Mougios, 2006). The second objective is to evaluate muscle uptake and metabolism of commercially available linoleate stable isotopes (ethyl $^{13}C_{18}$ -18:2n-6, NEFA $^{13}C_{18}$ -18:2n-6 and ethyl $^{2}H_{5}$ -18:2n-6) in soleus, red and white gastrocnemius muscle 8 h after a single oral dose while validating a novel internal isobutane GC-MS ion trap technique. The third objective will utilize a multiple simultaneous stable isotope design using $^{13}C_{18}$-18:2n-6, $^{2}H_{5}$-18:3n-3, $^{13}C_{16}$-16:0 and $^{2}H_{2}$-18:1n-9 to examine PUFA distribution in contrast to saturated and monounsaturated fatty acid distribution in soleus, red gastrocnemius, white gastrocnemius and heart muscle at 8h, 24h and 48h. In addition we will examine the accumulation of longer chain fatty acids derived from 18:2n-6 and 18:3n-3, in particular 20:4n-6 and 22:6n-3. It is also our intention to extend fatty acid composition and stable isotope analyses to individual lipid class fractions (TG, PL and NEFA) in order to gain better insights to the main depository destination for each PUFA inside the muscle.

In order to accomplish these objectives it was necessary to first develop an ion trap GC-MS method for analysing stable isotopic fatty acids and to evaluate its sensitivity to ^{13}C- and ^{2}H-labelled fatty acids. Fatty acid stable isotopes are currently considered the as gold standard technique for examining fatty acid metabolism in tissue but GC-MS fatty acid tracer analyses in

the literature have predominantly used transmission quadrupole GC-MS techniques followed by GC combustion IRMS. Initial efforts in method development included duplicating a common transmission quadrupole GC-MS method (Lin and Salem, Jr., 2007) with chemical ionization techniques using the ion trap GC-MS in external mode, followed by the development of a novel positive chemical ionization method using isobutane with the GC-MS in internal mode.

3.3 HYPOTHESIS

- Concentration of the endogenous pools of 18:2n-6, 18:3n-3, 20:4n-6 and, 22:6n-3 will be significantly higher in soleus as compared to that from red and white gastrocnemius muscles which will exhibit similar concentrations.
- Ethyl ester form of $^{13}C_{18}$-18:2n-6 will be the most cost and dose effective form of linoleate stable isotope.
- Preferential accumulation of the labelled 18:2n-6 and 18:3n-3 will occur in the order of soleus > red gastrocnemius > white gastrocnemius.
- Significantly higher amount of n-6 and n-3 isotopic labelled metabolites will be detected in soleus relative to that of red and white gastrocnemius which will exhibit similar behaviour.

CHAPTER 4

METHODS

4.1 Study Design

After establishing a GC-MS ion trap method with the sensitivity to detect the isotopic fatty acids in various skeletal muscle types, two separate tracer studies were designed to achieve the main objectives of this thesis. In the first tracer study known as "**linoleate study**" male Sprague-Dawley rats were obtained from Harlan Laboratories (Indianapolis, IN) at the age of 3 weeks and maintained under conventional conditions with controlled temperature (22°C) and illumination (12 h; 6:00 AM to 6:00 PM). After having been fed on Harlan Teklad 8640 rodent diet (**Table 4**) ad libitum with free access to water for 10 days, they were randomly assigned into four groups (n = 4/group), fasted overnight and administered a single oral bolus (0.15 mg/g body weight; ~ 20.4 mg) of one of the three stable isotopic linoleate; $^{13}C_{18}$-18:2n-6 EE,$^{13}C_{18}$-18:2n-6 NEFA and $^{2}H_{5}$ 18:2n-6 EE mixed in 0.48 mL of olive oil and only the vehicle oil was given to the control group. Animals were then returned to their cages for 8 h, where they had normal access to food and water. At the end of the experimental period, animals were anesthetised by an intraperitoneal pentobarbital sodium (30 mg/kg) injection and soleus, red gastrocnemius, and white gastrocnemius muscles were carefully excised with visible adipose tissue and fascias removed and immediately frozen in liquid nitrogen and stored at -80 °C for later analysis. Rats were euthanized by exsanguination followed by removal of the heart. A schematic diagram of the linoleate study is depicted in **Figure 5A**. As mentioned previously the purpose of the linoleate study was to evaluate muscle uptake of the available linoleic acid stable isotopes 8 h after oral gavage. The design for the second tracer study known as the "**MESSI study**" was

similar to the linoleate study except for the following; 1) twenty five male rats were used (n=5/group), 2) 8, 24 and 48 h time points were included, and 3) a mixture of four labelled fatty acids ($^{13}C_{18}$-18:2n-6, $^{2}H_{5}$-18:3n-3, $^{13}C_{16}$-16:0, and $^{2}H_{2}$-18:1n-9) were given (0.15 mg/g body weight; ~ 20.4 mg). For example, one dose would have 20 mg of every stable isotopic fatty acid which adds up to 80 mg of total stable isotopic fatty acid in addition to 0.4 mL of olive oil. A schematic diagram of the MESSI study is depicted in **Figure 5B**.

Finally in order to compare the concentration of endogenous pools of fatty acids among various muscle types, part of the muscle samples (i.e. soleus, red gastrocnemius, and white gastrocnemius muscles) from the control animals in the linoleate and MESSI study were subjected to the fast GC-FID analysis.

Table 4. Fatty acid composition of Harlan Teklad 8640 rodent diet.

Fatty Acid	Relative Composition (%)	Fatty Acid	Relative Composition (%)
14:0	0.5	18:2 n-6	46.6
16:0	14.7	20:4 n-6	0.04
18:0	4.6	Total n-6 PUFA	47
Total SFA	20.1		
		18:3 n-3	5.1
18:1 n-9	20.7	20:5 n-3	0.3
Total MUFA	23.5	22:6 n-3	0.2
		Total n-3 PUFA	5.7

SFA; saturated fatty acids; MUFA; mono-unsaturated fatty acids; PUFA; polyunsaturated fatty acids.

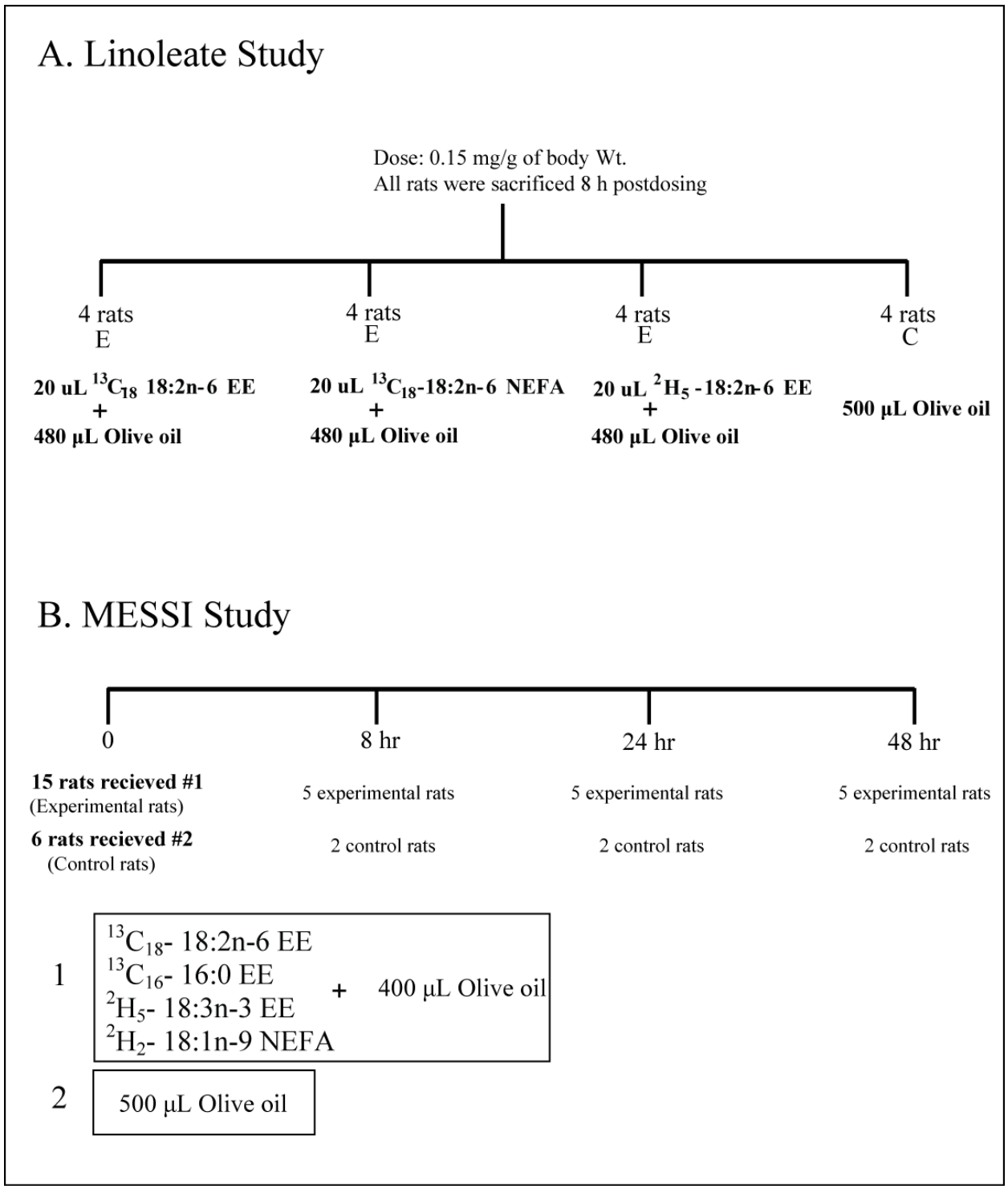

Figure 5. Schematic diagram of A) Linoleate study and B) MESSI study. E; experimental, C; control.

4.2 Isotope and Chemicals

Deuterium-labelled ethyl linoleate ($^{2}H_5$-17,17,18,18,18-18:2n-6 EE), carbon-13-uniformly labelled ethyl linoleate ($^{13}C_{18}$-18:2n-6 EE), deuterium-labelled ethyl linolenate ($^{2}H_5$-17,17,18,18,18-18:3n-3 EE), carbon-13-uniformly labelled ethyl palmitate ($^{13}C_{16}$-16:0) and deuterium-labelled nonesterified oleic acid ($^{2}H_2$-9,10-18:1n-9 NEFA) were obtained from Cambridge Isotope Laboratories (Andover, MA); isotope purities were > 98%, >96%, >90%, >95% and >98% respectively. Carbon-13-uniformly labelled nonesterified linoleate (U-13C-18:2n-6 NEFA) was obtained from Spectra Stable Isotope Inc., (Columbia, MD); isotope purity was > 98%. Unlabelled commercial reference standard 462 and unlabelled fatty acids were purchased from Nu-Chek Prep Inc., (Elysian, MN).

4.3 Homogenization, Lipid Extraction and Derivatization Reactions

Muscle samples were thoroughly diced at 4°C and disrupted in 2 mL methanol containing 0.01% butylated hydroxytoluene with a polytron homogenizer (Fisher Scientific, Hampton, NH). A known amount (~50ug/sample) of internal standard (17:0, 19:0 or 22:3n-3) was added to each sample prior to the homogenization. Total lipids were extracted from muscle homogenate (Bligh and Dyer, 1959) followed by direct transmethylation using 14% boron trifluoride (BF_3) in methanol (Morrison and Smith, 1964) as modified to include hexane (Salem, Jr., Reyzer, and Karanian, 1996).

4.4 GC-MS Analysis of the Stable Isotope Fatty Acids

A Varian 4000 Ion Trap GC-MS system (Varian Canada Inc., Mississauga, ON) was used for the quantification of fatty acid stable isotopes. An aliquot of 1 µL of FAMEs per sample was

injected using a Combipal autoinjector (CTC Analytics AG, Switzerland, Zwingen) onto a DB-FFAP 60m x 0.25mm i.d. x 25um film thickness, capillary column (J&W Scientific from Agilent Technologies, Mississauga, ON). The column was interfaced directly into positive chemical ionization (PCI) system using isobutane as the reagent gas with helium as the carrier gas. The GC oven temperature was programmed from 50°C to 130°C at the rate of 30°C/min followed by an 8°C/min ramp to 175°C, a 1°C/min ramp to 210°C, and a 30°C/min ramp to 245°C with a 30 min hold at the end. The injector and transfer line temperatures were maintained at 260°C and 250°C, respectively. Source temperature and manifold temperatures were 180°C and 50°C, respectively. Selected ion monitoring was carried out both for precursors and the main metabolites, using ions presented in **Table 3**. To reduce fragmentation and increase the level of control over sample ionization by chemical ionization, the instrumental parameters were set to allow mass-selected ion/molecule reaction to occur. With isobutane as the reagent gas, several reactant ions are produced including m/z 41, 43, 56, and 57, corresponding to $[C_3H_5]^+$, $[C_3H_7]^+$, $[C_4H_7]^+$, and $[C_4H_9]^+$ respectively. However, only $[C_4H_9]^+$ ions which chiefly result in proton transfer (i.e. $[MH]^+$ ion) were allowed to react with the sample molecules.

4.5 Fast GC Analysis

To quantify the endogenous pools of fatty acid in various muscle types fast GC-FID analysis (Masood and Salem, Jr., 2008; Masood, Stark, and Salem, Jr., 2005) was performed on a Varian 3900 system using a DB-FFAP of 15m × 0.1 mm ID × 0.1 µm film thickness (J&W Scientific from Agilent Technologies, Mississauga, ON). For the fast GC analysis, the temperature program included an initial temperature of 150°C with a 0.25 min hold followed by a 35°C/min ramp to 200°C, a 8°C/min ramp to 225 with 3.2 min hold, and then 80°C/min ramp to 245°C with 2.75 min hold. Carrier gas was H_2 at a flow rate of 0.5 ml/min with constant head

pressure of 344.7 kPa, and a split ratio of 100:1. The FID was set at 250°C with air and nitrogen make-up gas flow rates of 300 ml/min and 25ml/min, and a sampling frequency of 80 Hz. The Combipal autosampler (CTC Analytics AG, Switzerland, Zwingen) was set to inject 1 µL volume. Total run time for a single sample was 23.25 min.

4.6 Thin Layer Chromatography (TLC) Analysis

The lipid classes were fractionated by TLC on plates (20 × 20 cm) coated with silica gel 60 A and thickness of 250 µm (Whatman International Ltd. Maidstone, UK) using heptane: ethyl ether: acetic acid (60:40:3, v/v/v) (Christie, 2003) as the developing solvent. TLC standards for the TG fraction (triheptadecanoin; Nu-Chek Prep Inc., Elysian, MN) and PL fraction (1,2-dihetadecanoyl-sn-glycero-3-phosphocholine; Avanti Polar Lipids Inc., Alabaster, AL) were added to one aliquot (300 µl) of the total lipid extract and the mixture was dried under nitrogen stream. Dried lipids were dissolved in 50 µl of chloroform prior to applying to the TLC plates. Following this procedure, the plates were placed in the developing solvent for approximately 45min. The plates were allowed to dry at room temperature and lipid bands were visualized under UV light after spraying with a 0.5% solution of dichlorofluorescein prepared in ethanol. The gel band corresponding to PL, TG and NEFA were scraped off the plate and transferred into screw cap glass tubes. Fatty acids were then transmethylated in the presence of 14% BF_3 in methanol (v/v) at 100°C for 1 h. The resulting methyl esters were extracted and analyzed by GC-MS to measure the isotopic signal present in different lipid fractions.

4.7 Standard Curves

4.7.1 Standard curves for isotopic precursor.

For each isotopic precursor stock solution, a series of serial dilution were made and a constant amount of internal standard (ISTD) 17:0 ethyl ester was added. The range of these samples covered the estimated range of isotope-labelled fatty acid in rat muscle samples. Standard curves were determined using linear regression of the ratio of signal areas between isotopes and ISTD versus the ratio of amounts between isotopes and ISTD

4.7.2 Standard curves for isotopic metabolites.

To estimate the slopes of the standard curves for the major isotopic metabolites for which stable isotope-labelled compounds were not available, the ratios of the slopes determined from the standard curves for the various precursors isotopomers (e.g. unlabelled 18:2n-6, $^{13}C_{18}$-18:2n-6, $^{2}H_{5}$-18:2n-6) were used as previously described (Lin, Pawlosky, and Salem, Jr., 2005). For example, to determine the standard curve for $^{13}C_{18}$-20:4n-6, it was assumed that the relationship of the slopes of unlabelled 18:2n-6 and $^{13}C_{18}$-18:2n-6 was the same as that of unlabelled 20:4n-6 and $^{13}C_{18}$-20:4n-6. The intercepts were generally very close to the origin and so are not specified.

4.7.3 Standard curves for the unlabelled fatty acids.

Stock solution of each unlabelled fatty acid were diluted into a series of working solutions with a range of 5-100 ng per sample with ISTD added to each sample. Both the isotope-labelled and unlabelled samples were processed similarly for GC-MS analysis.

4.8 Statistical Analysis

Statistical analyses were performed using GraphPad Prism (Version 4, GraphPad Software Inc., San Diego, CA) and SPSS (Version 16.0, SPSS Inc., Chicago, IL). All values are expressed as means ± SEM. To compare the differences in endogenous pools of fatty acids among various muscle types one-way ANOVA was conducted with Tukey's honestly significantly difference test as the post hoc test. The potential for significance was inferred at $P < 0.05$. All statistical analyses associated with both linoleate and MESSI study were two-way ANOVA in conjunction with the appropriate post hoc test to determine the significant differences between the individual means. In the linoleate study, 18:2n-6 isotope and tissue effects were examined, and in the MESSI study, tissue and time effects were examined. Significance was inferred at $P < 0.05$. A least-squares linear fitting procedure was used to determine the standard curves of isotopic and unlabelled fatty acids. When the regression coefficient was ≥ 0.95, it was considered to be an acceptable fit of the data to the regression.

CHAPTER 5

RESULTS

5.1 Comparison of Endogenous Pools of Fatty Acids in Various Muscle Types

Fatty acid composition of total lipid extracts from soleus, red gastrocnemius, white gastrocnemius and heart were expressed in concentrations (**Table 5**) and relative mole percentages (**Table 6**). Total fatty acid concentrations were significantly higher (~ 2-fold) in soleus as compared with red and white gastrocnemius which exhibited similar concentrations. These differences were mainly a result of much higher concentration of total monounsaturates (over 3-fold), but total saturates, total PUFA and total n-6 PUFA concentrations in soleus were also significantly higher. Nonetheless, concentrations of HUFA in soleus did not differ from red and white gastrocnemius. Concentrations of fatty acids in heart were similar to that of soleus, except for a significantly higher HUFA and total n-3 PUFA. When fatty acids were expressed as relative mole percentages, the fatty acid composition of soleus tended to resemble white gastrocnemius in total PUFA, total n-6 PUFA and total n-3 PUFA, however the proportions of total saturates and total HUFA were significantly lower in soleus compared to white gastrocnemius. In contrast, proportions of total monounsaturates in soleus were significantly higher than white gastrocnemius. As compared to red gastrocnemius, soleus had significantly lower percentages of total PUFA and subclasses of PUFA including total n-3 PUFA and total HUFA. In regard to total saturates and total monounsaturates, red gastrocnemius composition was similar to white gastrocnemius as compared to soleus. Interestingly, proportions of fatty acids in heart muscle are in close agreement with that of red gastrocnemius.

The fatty acid composition also varied at the level of the individual fatty acids. Most importantly, both concentrations and proportions of 18:2n-6 and 18:3n-3 were significantly higher in soleus as compared with red and white gastrocnemius muscle which exhibited similar values. Heart content of 18:2n-6 and 18:3n-3 were similar to those of red and white gastrocnemius muscles. Although soleus and gastrocnemius muscles showed similar concentration of 20:4n-6, the proportions of this fatty acid were significantly higher in red and white gastrocnemius relative to soleus. Heart concentrations of 20:4n-6 along with its proportions were significantly higher (~ 2 fold in concentration and 1.5 fold in mole percentage) relative to the skeletal muscles. In regard to 22:6n-3, soleus resembled red gastrocnemius in concentrations which were significantly higher than white gastrocnemius 22:6n-3 concentrations. In term of relative mole percentages of 22:6n-3, soleus had similar percentages as white gastrocnemius and both showed higher proportions compared to red gastrocnemius. While heart concentration of 22:6n-3 was higher than all skeletal muscles, there were no differences as compared with red gastrocnemius when DHA was expressed as relative mole percentage.

5.2 Linoleate Study

5.2.1 Fibre type-specific uptake of deuterium-and carbon-13-labelled linoleate

The accretion of the linoleate tracer in specific muscle types is expressed as net accumulation (nmol/g of muscle, **Figure 6A**) and percent enrichment (concentration of labelled linoleate/concentration of endogenous pool of linoleate, **Figure 6B**). The net accumulation of NEFA and EE forms of ^{13}C labelled linoleate among various muscle types were in the order of soleus > red gastrocnemius = white gastrocnemius ($P < 0.05$). Similar rank order was observed for that of ^{2}H labelled linoleate (EE only) however, the differences between the muscle types did

not reach significance. There was a good agreement between the net accumulation data with that of percent enrichment (**Figure 6A** and **6B**), which further postulates the muscle type discrepancy in linoleate uptake and metabolism. Complementary to these results, the total amount of labelled linoleate in each muscle type was also expressed as the percentage of total precursor dose (**Table 7**). The greatest percentage of the total precursor dose was observed in red gastrocnemius as NEFA ^{13}C labelled linoleate (0.028 %) while ^{2}H -labelled linoleate in both soleus and white gastrocnemius muscle was the lowest (0.002 %). The results from EE form of ^{13}C labelled linoleate were in agreement with that of NEFA.

5.2.2 Fibre type-specific distribution of deuterium and carbon-13-labelled linoleate derived metabolites in vivo 8 h post dosing

Similar to the labelled precursor, the results from the distribution of deuterium and carbon-13-labelled linoleate derived metabolites *in vivo* 8 h after dosing were expressed in two units; nmol/g of muscle, and the percentage of the endogenous pool (**Table 8**). The principle n-6 metabolites derived from labelled linoleate were 20:3n-6 ($^{13}C_{18}$-20:3n-6 or $^{2}H_{5}$-20:3n-6) and 20:4n-6 ($^{13}C_{18}$-20:4n-6 or $^{2}H_{5}$-20:4n-6). Soleus had significantly higher concentration of $^{13}C_{18}$-20:3n-6 relative to the gastrocnemius muscles ($P < 0.05$). Consistently, $^{13}C_{18}$-20:4n-6 was solely detected in soleus and its concentration was in a close range with that of $^{13}C_{18}$-20:3n-6. It is important to note that the levels of labelled metabolites in white gastrocnemius were undetectable. Expressing the labelled metabolites data as the percentages of total precursor dose was not informative since the percentages were found to be very negligible and similar among various muscle types.

5.2.3 Efficacy of deuterium and carbon-13 isotopes in tracing labelled linoleate in specific muscle types 8 h after single oral dose.

$^{13}C_{18}$-18:2n-6 (EE or NEFA) and $^{2}H_{5}$-18:2n-6 are 18 and 5 atomic mass unit (amu) higher than the mass of unlabelled 18:2n-6 (295 amu) respectively. Likewise, metabolic products of these isotopic fatty acids carry the same mass differences as their corresponding tracer. Consistently higher amounts of ^{13}C labelled precursor molecule was detected in all muscle types relative to that labelled with ^{2}H, however this difference only reached significance when the NEFA form of $^{13}C_{18}$-18:2n-6 was compared with $^{2}H_{5}$-18:2n-6 EE (**Figure 6A&B**). In agreement with the later finding, no isotopic metabolites were detected for the ^{2}H-labelled precursor in any of the muscle types examined (**Table 8**). It is noteworthy that there were no significant differences between NEFA and EE forms in distribution, desaturation and chain-elongation across muscle types.

5.3 MESSI Study

5.3.1 Time-course of $^{13}C_{18}$-18:2n-6 and its major metabolites in various muscles

The appearance and disappearance of $^{13}C_{18}$-18:2n-6 and its major *in vivo* metabolites among various muscle types after a single oral dose are presented in **Figures 7-9**. The n-6 precursor was at its maximal concentration (C_{max} in nmol/g) at the first experimental time point of 8 h in soleus (95), heart (35), red gastrocnemius (22) and white gastrocnemius (18) and decreased sharply in heart and red gastrocnemius, while in soleus and white gastrocnemius it decayed slowly over the course of the study (See **Figure 7**). It is noteworthy that the net concentration of $^{13}C_{18}$-18:2n-6 in soleus was significantly greater than that in other muscle types.

Red gastrocnemius, white gastrocnemius and heart muscles exhibited similar net concentration of $^{13}C_{18}$-18:2n-6.

The appearance and disappearance patterns of $^{13}C_{18}$-20:3n-6 and $^{13}C_{18}$-20:4n-6 were different from that of $^{13}C_{18}$-18:2n-6. $^{13}C_{18}$-20:3n-6 was present in all muscle tissues at 8 h and it gradually accumulated in all muscle types throughout the experimental period except for white gastrocnemius in which the $^{13}C_{18}$-20:3n-6 accretion (0.2 nmol/g) was halted at 24 h and it began to decline slowly thereafter (**Figure 8**). Therefore, the $^{13}C_{18}$-20:3n-6 C_{max} values for soleus (1.8 nmol/g), heart (0.7 nmol/g) and red gastrocnemius (0.3 nmol/g) were all achieved at 48 h with soleus net concentration of $^{13}C_{18}$-20:3n-6 being significantly higher than that of other muscle groups. $^{13}C_{18}$-20:4n-6 was detected in soleus at 8, 24 and 48 h (C_{max} = 8.0 nmol/g at 48h) but was detected in red gastrocnemius at 8 h only (C_{max} = 3.5 nmol/g), in heart at 48 h only (C_{max} = 8.0 nmol/g) and was not detected in white gastrocnemius at any time point (**Figure 9**).

5.3.2 Time-course of $^{2}H_5$-18:3n-3 and its major metabolites in various muscles

The appearance and disappearance of $^{2}H_5$-18:3n-3 and its major *in vivo* metabolites among various muscle types after a single oral dose are presented in **Figure 10-12**. Similar to the n-6 precursor, $^{2}H_5$-18:3n-3 was also at its maximal concentration at 8 h in heart (20 nmol/g), red gastrocnemius (15 nmol/g) and white gastrocnemius (7 nmol/g), and decreased sharply by 24 h, particularly in heart and red gastrocnemius and remained low at 48 h in all tissues (**Figure 10**). $^{2}H_5$-18:3n-3 rapidly accumulated in soleus by 8 h however, unlike the other muscle groups, $^{2}H_5$-18:3n-3 continued to increase and reached its C_{max} (23 nmol/g) at 24 h and remained relatively high at 48 h. Therefore at 24 and 48 h, soleus had significantly higher concentrations of $^{2}H_5$-18:3n-3 than the other muscle tissues which exhibited concentrations similar to each other.

The accumulation of $^{2}H_5$-20:5n-3 and $^{2}H_5$-22:6n-3 followed a different pattern. $^{2}H_5$-20:5n-3 was not detected in soleus at any time point, while it was detected in all remaining muscles at 8 h (**Figure 11**). $^{2}H_5$-20:5n-3 was maximal in white gastrocnemius at 8 h (0.5 nmol/g) with a subsequent decline at 24 h and no detectable $^{2}H_5$-20:5n-3 at 48 h. In red gastrocnemius $^{2}H_5$-20:5n-3 was similar at 8 h and 24 h with a subsequent decline by 48 h. Unlike the skeletal muscles, heart continued to accumulate $^{2}H_5$-20:5n-3 throughout the 48 h period. The observed concentrations for $^{2}H_5$-22:6n-3 were almost 10-fold higher than that of $^{2}H_5$-20:5n-3. $^{2}H_5$-22:6n-3 reached a maximal accumulation in the soleus at 8 h followed by a rapid disappearance by 24 h that persisted to 48 h (**Figure 12**). In heart and red gastrocnemius, the concentrations of $^{2}H_5$-22:6n-3 tended to increase over the 48 h, while $^{2}H_5$-22:6n-3 was not detected in white gastrocnemius.

5.3.3 Time-course of $^{13}C_{16}$-16:0 and $^{2}H_2$-18:1n-9 distribution in various muscle types

$^{13}C_{16}$-16:0 and $^{2}H_2$-18:1n-9 1 were included in our study to compare the sensitivity of our analytical method with previous studies and to examine differences between the polyunsaturates as compared with saturates and monounsaturates.

Consistent with the n-6 and n-3 precursors, $^{13}C_{16}$-16:0 and $^{2}H_2$-18:1n-9 were detected by 8 h after dosing with $^{2}H_2$-18:1n-9 reaching maximal concentration in all muscles at 8h (**Figure 13**) and $^{13}C_{16}$-16:0 in soleus, red gastrocnemius and white gastrocnemius reached maximal concentrations at 24 h although the concentrations at 8 h were 90-95 % of these maximums (**Figure 14**). In heart, the maximal concentration of $^{13}C_{16}$-16:0 was reached at 8 h. Skeletal muscles maintained a high level of $^{13}C_{16}$-16:0 throughout the 48 period while in heart muscle it reached a plateau after a sharp decrease at 24 h. In contrast, $^{2}H_2$-18:1n-9 was completely

eliminated from red gastrocnemius and heart muscle after 8 h, while in the soleus and white gastrocnemius it was maintained at a relatively consistent level.

5.3.4 Compartmentalization of labelled fatty acids among various lipid classes

Due to the analyzing capacity of the GC-MS system in detecting tracer molecules, only precursor fatty acids which exhibited the most abundance of isotopic signal at the 8 h time point were subjected to the lipid fractionation analysis. Thus, the distribution of $^{13}C_{18}$-18:2n-6, $^{2}H_{5}$-18:3n-3, $^{13}C_{16}$-16:0 and $^{2}H_{2}$-18:1n-9 among PL, TG and NEFA fractions are plotted in **Figure 15**. Most of the $^{13}C_{18}$-18:2n-6 signal was found among TG fraction accounting for 50-65% of the signal in red and white gastrocnemius muscle (20-35% in PL fraction) and ~ 80% of that in soleus (~ 10% in PL fraction). A small quantity of $^{13}C_{18}$-18:2n-6 (~ 1-10 %) was also detected in NEFA fraction. Similar to the n-6 precursor, TG fractions were the main repository compartment for $^{2}H_{5}$-18:3n-3 however they accommodated ~ 80% of signal in red and white gastrocnemius as compared to ~ 45% in soleus. Compartmentalization of $^{13}C_{18}$-18:2n-6 and $^{2}H_{5}$-18:3n-3 among various lipid classes in heart muscle showed similar pattern as red and white gastrocnemius muscles.

$^{13}C_{16}$-16:0 showed a muscle type specific distribution pattern. In red gastrocnemius $^{13}C_{16}$-16:0 was equally distributed among various lipid classes. In white gastrocnemius, the PL fraction became the main repository compartment (> 60%) with TG and NEFA fractions sharing the remnant $^{13}C_{16}$-16:0 signal equally. In the soleus, the $^{13}C_{16}$-16:0 signal was mainly incorporated into TG, followed by PL with little signal in NEFA, a distribution similar to that of $^{13}C_{18}$-18:2n-6 in soleus. In heart muscle, TG, PL and NEFA each accumulated 45, 30, and 25 % of the total $^{13}C_{16}$-16:0 signal, respectively.

For $^{2}H_{2}$-18:1n-9 in red gastrocnemius and heart, > 50% of the $^{2}H_{2}$-18:1n-9 was accreted in the NEFA fraction, ~ 25-40% in the TG fraction and a small quantity was detected in the PL fraction. In the soleus and white gastrocnemius, the TG fraction was the principle depot as it accumulated 75 to 90% of the $^{2}H_{2}$-18:1n-9, while levels in both the NEFA and PL fractions were minor.

CHAPTER 6

DISCUSSION

6.1 Comments on hypotheses

1. *Concentration of the endogenous pools of 18:2n-6, 18:3n-3, 20:4n-6 and 22:6n-3 will be significantly higher in soleus as compared to that from red and white gastrocnemius muscles which will exhibit similar behaviour.*

A systematic comparison of fatty acid compositions in soleus, red gastrocnemius and white gastrocnemius revealed significantly higher concentrations of 18:2n-6 and 18:3n-3 in soleus relative to that from red and white gastrocnemius which were similar. Although the concentration of the endogenous pools of 20:4n-6 and 22:6n-3 were higher in soleus as compared with red and white gastrocnemius muscles, the difference did not reach significance. The concentration of total fatty acids was significantly higher in soleus as compared with red and white gastrocnemius which exhibited similar concentrations. These differences were a result of much higher concentrations of total monounsaturates (over 3-fold), total saturates, total PUFA and total n-6 PUFA concentrations in soleus.

2. *Ethyl ester form of $^{13}C_{18}$-18:2n-6 will be the most cost and dose effective form of linoleate stable isotope.*

Results from linoleate study conclusively demonstrated that uniformly labelled carbon-13 isotopes are the most effective form of stable isotopes to be employed in fatty acid tracer studies in small muscle samples as compared to those labelled with deuterium. With regard to the ester bonds, NEFA form of labelled fatty acids resulted in slightly higher isotopic signal as compared

to that of EE. However, since the difference was not found significant it was decided to carry on with the EE form to match with the large body of tracer studies which use EE form (Lin, Pawlosky, and Salem, Jr., 2005; Lin and Salem, Jr., 2007; Lin and Salem, Jr., 2005).

3. *Preferential accumulation of the labelled 18:2n-6 and 18:3n-3 will occur in the order of soleus > red gastrocnemius > white gastrocnemius.*

According to the results collected in our tracer studies, soleus was unequivocally the predominant muscle type in accumulating 18:2n-6 and 18:3n-3 followed by red gastrocnemius and white gastrocnemius. However, despite a slight elevation in the concentration of the labelled n-6 and n-3 precursors in red gastrocnemius compared to white gastrocnemius, the behaviour of the two portions of gastrocnemius muscle was not found significantly different from one another. The results from deuterium labelled isotopes also agree with the above findings.

4. *Significantly higher amounts of n-6 and n-3 isotopic labelled metabolites will be detected in soleus relative to that of red and white gastrocnemius which will exhibit similar behaviour*

Significantly higher concentrations of n-6 stable isotopic metabolites (20:3n-6 and 20:4n-6) were detected in the soleus relative to red and white portion of gastrocnemius muscle, as confirmed with both the linoleate and MESSI study. The behaviour of the red and white gastrocnemius muscle in accumulating isotopic n-6 metabolites was elusive relative to one another and across the two studies. However, this matter is discussed later in more detail. With regard to the n-3 metabolites which were examined only in MESSI study, labelled 20:5n-3 was undetectable in soleus throughout the 48 h period while in red and white gastrocnemius muscles relatively high amounts of 20:5n-3 at 8 and 24 h were detected. For the 22:6n-3, soleus accreted a higher amount of this labelled n-3 metabolite at 8 h after dosing as compared with red

gastrocnemius. At 24 and 48 h, labelled 22:6n-3 was not detected in soleus, while labelled 22:6n-3 increased in red gastrocnemius. Labelled 22:6n-3 was not detected in white gastrocnemius throughout the study.

6.2 Effect of Fibre Type Composition on PUFAs Distribution in Various Muscle Types

To our knowledge, no previous study has attempted to systematically follow PUFAs distribution among various muscle types with discrete fibre type composition. In two separate tracer studies conducted in our laboratory, it was established that PUFAs distribution varies among different muscle types ultimately due to their distinct fibre type composition. We analyzed soleus, red and white gastrocnemius muscles which have been examined in numerous studies as the muscle groups with distinct fibre type composition (Blackard et al., 1997; Gorski, Nawrocki, and Murthy, 1998; Kriketos et al., 1995; Nikolaidis, Petridou, and Mougios, 2006). The main reason behind the inclusion of heart muscle in some of the analyses was to provide a measure for a direct comparison between the efficiency of our mode of administration and analytical system with that published in Salem laboratory (Lin and Salem, Jr., 2007).

6.2.1 Fibre type-specific distribution of n-6 and n-3 precursors

Concentration (nmol/g of tissue) results from both deuterium and carbon-13-labelled linoleate consistently revealed that soleus was the predominant muscle type in accumulating significantly higher concentration of labelled linoleate as compared with red and white gastrocnemius which were similar. Rendering the concentration results to percent enrichments (i.e. concentration of labelled 18:2n-6 / concentration of endogenous pool of 18:2n-6) also brought about the same rank order; soleus > red gastrocnemius = white gastrocnemius. $^{2}H_{5}$18:3n-3 distribution similarly resulted in higher accumulation of this tracer in soleus as compared with

red and white gastrocnemius. In most part, heart muscle closely resembled gastrocnemius muscles in accretion of n-6 and n-3 precursors. The concentration results from the heart muscle were in close agreement with those reported previously (Lin and Salem, Jr., 2007). Differences in blood flow to each muscle type at rest, discrepancy in FAT/CD 36 expression levels and disparity in LPL activity, all induced by fibre type compositions, are three possible explanations for this trend of labelled n-6 and n-3 precursor uptake among various muscle types. It has been shown that when the rats are standing, blood flow is highest in muscles containing large proportions of type I fibres (e.g. soleus muscle; 86% type I, (Delp and Duan, 1996). It was also suggested that type I fibres and to a lesser extent type IIA fibres (e.g. red gastrocnemius; 55% type I and 31% type IIA, (Delp and Duan, 1996) are the primary types of fibres recruited during postural maintenance. As the rats begin to walk at 15 m/min, there is a close relationship between the increase in blood flow above rest and population of recipient type IIA fibres in muscles. Type IIB fibres (e.g. white gastrocnemius; 95% type IIB (Delp and Duan, 1996) had a negligible blood supply until the rats were running at the moderate intensity of 60 m/min (Armstrong and Laughlin, 1985; Delp et al., 1991; Laughlin and Armstrong, 1983). Since the rats in our study were kept in small cages throughout the study one can speculate that soleus uptake of labelled linoleate and linolenate may be partially due to its markedly higher blood supply as compared with red and white gastrocnemius muscles (Delp et al., 1991). A high level of fat transporters (i.e. FAT/CD 36) in the soleus plasma membrane, and high LPL activity in soleus capillary beds also supports a high uptake of labelled fatty acids by the soleus. LPL activity and FAT/CD 36 expression have been shown to be fibre type specific with being highest in red muscle and lowest in white muscle (Bonen et al., 1998; Smol et al., 2001).

The marked difference in 18:2n-6 and 18:3n-3 uptake and incorporation between soleus and gastrocnemius muscles appears to be associated with the endogenous pool of these fatty acids within these specific tissues. In the present study 18:2n-6 and 18:3n-3 content of soleus were found 2-fold and 5-fold, respectively, greater than red and white gastrocnemius which had similar concentrations that agrees with previous reports (Blackard et al., 1997; Gorski, Nawrocki, and Murthy, 1998; Kriketos et al., 1995; Nikolaidis, Petridou, and Mougios, 2006). Therefore, the high concentration of labelled n-6 and n-3 precursors in soleus is likely due to specific requirements and/or larger endogenous pools (TG and PL) for these fatty acids. This may be a result of different rates of uptake, retention or partitioning away from β-oxidation in the soleus as compared with other muscles. With regard to behaviour of the heart muscle, it is important to mention that the endogenous concentrations of 18:2n-6 and 18:3n-3 in this tissue were near those found in red and white gastrocnemius muscle. However further elaboration on the heart uptake of labelled n-6 and n-3 precursors compared to the skeletal muscle is beyond the scope of this document.

6.2.2 Fibre type-specific distribution of n-6 and n-3 metabolites

As it was expected from the labelled 18:2n-6 results, soleus was labelled with significantly higher concentrations of the principle n-6 metabolites (20:3n-6 and 20:4n-6) relative to red and white gastrocnemius muscles. Interestingly, concentrations of labelled 20:3n-6 in various muscle types were markedly lower (up to 10 fold) than that of labelled 20:4n-6. Conversely, in previous human (McCloy et al., 2004) and animal (Lin and Salem, Jr., 2007) studies, concentrations of labelled 20:4n-6 derived from labelled linoleate was always dominated by that of 20:3n-6 in the circulation consistent with the sequence of metabolic reactions. The reported enrichment patterns (i.e. ~ 10-fold higher amount of 20:3n-6 than 20:4n-6) of the n-6

metabolites in the plasma (McCloy et al., 2004) which were opposite to what was found in our study in the muscles, have led us to believe that the primary accretion mechanism for the labelled 20:3n-6 and 20:4n-6 has been through local metabolism of the labelled linoleate inside muscle rather than the uptake of the preformed molecules from circulation. After cloning of human Δ6 desaturase (rate-limiting enzyme in catalyzing the conversion of 18:2n-6 into 20:3n-6 and 20:4n-6), cDNA northern analysis revealed that it is expressed not only in liver but in a variety of human tissues including muscle (Cho, Nakamura, and Clarke, 1999). To our knowledge, there has not been a study to compare the activity or the expression of Δ6 desaturase enzyme in various muscles types. Alternatively, incorporation of 20:3n-6 and 20:4n-6 into specific PL and other lipid classes may be affected by the endogenous pools of these lipid classes and the turnover kinetics for these PUFAs in each specific muscle.

An *in vitro* study of cultured lung fibroblasts using ^{14}C-labelled fatty acids showed that 20:3n-6 and 20:4n-6 were incorporated differentially into various PL species, with 20:3n-6 enriched in phosphatidylethanolamine and phosphatidylglycerol, and 20:4n-6 enriched in phosphatidylcholine (Weithmann, Peterson, and Sevanian, 1989). Similarly in rat liver microsomes, 20:3n-6 was incorporated mainly into phosphatidylcholine, phosphatidylethanolamine, and phosphatidylinositol, and 20:4n-6 occurred primarily in phosphatidylinositol (Garda et al., 1997; Shimada, Morita, and Sugiyama, 2003). However, there has been yet a study to explore the differential incorporation of PUFAs in specific PL classes in muscle tissue. It has been demonstrated that in both the SR and mitochondria, phospholipids consist of approximately 80% of total lipids, with phosphatidylcholine and phosphatidylethanolamine making up to70-75% of the PL fraction (Fiehn et al., 1971). Considering the differential incorporation of PUFAs into phosphatidylethanolamine and

phosphatidylcholine, differences in PUFAs distribution, incorporation and metabolism among muscle types with varying degree of SR and mitochondrial content is probable.

Despite the dramatic disparities in the distribution of labelled n-6 metabolites among the examined skeletal muscle types, fatty acid composition results from our study and previous studies (Blackard et al., 1997; Gorski, Nawrocki, and Murthy, 1998; Kriketos et al., 1995; Nikolaidis, Petridou, and Mougios, 2006) showed similar concentrations of 20:3n-6 and 20:4n-6 among soleus, red and white gastrocnemius. The distribution pattern of the labelled n-3 was somewhat different from the labelled n-3 precursor. Red gastrocnemius was the main repository compartment for the labelled 20:5n-3 while soleus was for that of labelled 22:6n-3. Unexpectedly, soleus was free from labelled 20:5n-3 and no detectable levels of labelled 22:6n-3 was found in white gastrocnemius. Labelled 20:4n-6 was also missing from white gastrocnemius. Similar to the n-6 metabolites, results from Cunnane (McCloy et al., 2004) and Salem (Lin and Salem, Jr., 2007) have led us to believe that the primary mechanism for the accumulation of the labelled n-3 metabolites in the examined skeletal muscle was the intramuscular metabolism of the labelled 18:3n-3. In regard to the endogenous concentrations of 20:5n-3 and 22:6n-3 in the muscle types, soleus and red gastrocnemius had similar concentration which in turn were significantly higher than that of white gastrocnemius. Heart muscle behaved very similar to red and white gastrocnemius in regards to accumulating both n-3 and n-6 metabolites. Heart results were in complete agreement with the literature (Lin and Salem, Jr., 2007).

6.2.3 Fibre type-specific distribution of labelled palmitate and oleate

The net concentration of labelled palmitate was significantly elevated in soleus as compared to red and white gastrocnemius. Soleus content of labelled oleate was also greater (up to 6 fold) than that of red and white gastrocnemius muscles. Due to the large level of uncertainty

in the $^{2}H_{2}$-18:1n-9 determinations, the difference between muscle types was not found to be significant. However, the labelled palmitate and oleate accretion in various muscle types closely agree with that of their endogenous pool size. The endogenous pool of 16:0 in soleus, although statistically significant, was only slightly higher from that of red and white gastrocnemius muscle. In comparison, the concentrations of unlabelled 18:1n-9 in soleus were ~ 5-fold higher from that of gastrocnemius muscles.

6.3 Changes in PUFAs Distribution Pattern as the Function of Time

Distinct and somewhat predictable distribution patterns emerged for the labelled PUFA precursors versus labelled PUFA metabolites. While the abundance of the labelled precursors, in all muscle types, gradually declined over the course of the study, the isotopic signal of the labelled metabolites increased over time. Maximal accretion of $^{13}C_{18}$-18:2n-6 and $^{2}H_{5}$-18:3n-3 occurred at 8 hr in all muscle types and it decayed thereafter. However, labelled 18:3n-3 disappeared faster than labelled 18:2n-6, particularly in the red gastrocnemius and heart muscles. The maximal concentration of deuterated 18:2n-6 observed in plasma, skeletal muscles and heart is at 8 h, while for 18:3n-3 maximal concentrations have been observed at 4 hour in plasma and 8 h in heart and liver (Lin and Salem, Jr., 2007). Similar to our results, the 18:2n-6 and 18:3n-3 concentrations began to decay immediately after their peak with a faster rate for 18:3n-3 compared to 18:2n-6. Time to peak enrichment has been shown to be significantly shorter for ^{13}C 18:3n-3 (6 h) than for the ^{13}C 18:2n-6 (8-10 h) (McCloy et al., 2004). The decay curve for ^{13}C in plasma total lipids occurred immediately after peak concentrations and was exponential, with ^{13}C 18:2n-6 having ~4-fold longer half-life than that of 18:3n-3. Appearance and disappearance rates were similar across the muscle types, therefore the rank order of labelled 18:2n-6 and 18:3n-3

concentrations in muscle types remained intact across time (i.e. soleus > red gastrocnemius = white gastrocnemius = heart).

According to the metabolic sequence of reactions, the intermediate n-6 (20:3n-6) and n-3 (20:5n-3) metabolites appeared in various tissues as early as 4 h post dosing and peaked at 24-96 h (Lin and Salem, Jr., 2007). However the major *in vivo* n-6 (20:4n-6) and n-3 (22:6n-3) metabolites were first detected at 24 h and were still increasing at the last time point studied (e.g. 600 h). Our results concerning the appearance and disappearance pattern of labelled 20:3n-6 is in accordance with the previously published results and there is no change in the rank order of the muscle types as a function of time. Although soleus and red gastrocnemius were rapidly labelled with a large concentration of 20:4n-6 at 8 h, this long chain n-6 PUFA was completely eliminated from red gastrocnemius thereafter, while it reached a higher concentration in soleus at 48 h subsequent to a decline at 24h. Similar changes have been reported in a mixed muscle sample (Lin and Salem, Jr., 2007). High concentrations of deuterium labelled n-6 metabolites observed at 4 and 8 h time points decreased to half of their concentrations by 24 h, but at 96 h the concentrations began to rise and reached their maximum at 360 h (Lin and Salem, Jr., 2007). Labelled 22:6n-3 accumulation also varied across the muscle types over the examined time points. Soleus accumulated labelled 22:6n-3 to the highest concentration at 8 h as compared with red gastrocnemius and heart. Labelled 22:6n-3 was no longer detectable in soleus at 24 and 48 h, but increasing 22:6n-3 concentrations were detected in red gastrocnemius and heart. Previous results in mixed muscle samples also indicate a pattern of substantial accumulation of labelled n-3 metabolites in the initial period (4 and 8 h) followed by a decline at 24 h and increasing accumulation at 96 h to a maximal concentration at 600 h (Lin and Salem, Jr., 2007).

Although the mechanism for appearance and disappearance patterns among various muscle types is not clear, the close agreement of between our results with previous results (Lin and Salem, Jr., 2007) in the heart muscle strongly suggests that our results are accurate measures of PUFA accumulation in specific muscle types.

6.4 Efficacy of Deuterium-and Carbon-13 isotopes

Our results concerning the quantitative recovery of ^{13}C-labelled linoleate among various rat skeletal muscle types agree with previous stable isotope studies (Lin and Salem, Jr., 2007; McCloy et al., 2004). The amount of $^{13}C_{18}$-18:2n-6 NEFA/EE tracers detected in soleus, red and white gastrocnemius ranging from 15 to 124 nmol/g of muscle were in close agreement with that of $^{2}H_{5}$-18:2n-6 EE found in heart muscle (~ 65 nmol/g of tissue) 8 h post dose (Lin and Salem, Jr., 2007). Previously, fatty acid profiles of heart muscle was found to be comparable to that of soleus (Nikolaidis, Petridou, and Mougios, 2006) with the linoleate content of heart and soleus determined as 24 ±8 versus 28 ±4 mol % in triacylglycerol fraction and 47 ± 2 versus 34±2 mol % in phospholipid fraction, respectively.

Unexpectedly, a lower amount of ^{2}H-labelled linoleate was measured in all muscle fibres compared to that labelled with ^{13}C, however the difference only reached significance when the comparison was made between the ^{13}C and ^{2}H tracer accumulated in soleus muscle. In contrast, it has been reported that the endogenous pools of fatty acids have a greater suppressing effect on the measurements of ^{13}C-labelled linoleate relative to that labelled with ^{2}H (Lin, Pawlosky, and Salem, Jr., 2005). It is assumed that the reduced ^{2}H signal in the present study is attributable to either the novel PCI quadrupole ion trap GC/MS technique which yet to be evaluated with this regard or simply a lower dose of ^{2}H tracer which may have been resulted from imprecision at the time of dosing. Nonetheless, the results from ^{2}H labelled linoleate strongly resembled that of ^{13}C

labelled linoleate in uncovering the fibre type differences in linoleate uptake and metabolism supporting the main objective of this study.

6.5 Efficacy of the Novel PCI GC-MS

The internal isobutane PCI technique was developed to minimize parent ion fragmentation, increase sensitivity, produce linear responses, and allow simple sample preparation. Fragmentation of all FAMEs was reduced compared to either EI or methane PCI. The methane and isobutane PCI methods did not differ much in the profiles of saturated FAMEs, but in isobutane PCI, all unsaturated FAMEs were significantly less fragmented, and all FAMEs showed some level of intact parent ion. As yet, no published work has documented the use of isobutane PCI for isotopic FAME analysis in a quadrupole ion trap. In most of the tracer studies referenced in this document (Lin, Pawlosky, and Salem, Jr., 2005; Lin and Salem, Jr., 2007), methane NCI analysis of the PFB ester fatty acids via the transmission quadrupole GC-MS system was employed for measuring stable fatty acid isotopes. However our experiments on NCI method using methane as the reagent gas have led us to believe that methane NCI may not be the most suitable method for measuring isotopic signal, especially in quadrupole ion trap systems. Our results gathered using the novel PCI method are in a close range with the previously published results using methane NCI in rat models with comparisons to the accretion of labelled 18:2n-6 and 18:3n-3 in heart tissue as validation. For instance the net accumulation of labelled 18:2n-6 and 18:3n-3 in heart tissue, documented in the MESSI study, were in the range of 20-40 and 5-20 nmol/g of tissue, respectively, while those reported previously (Lin and Salem, Jr., 2007) were in the range of 35-65 and 10-25 nmol/g of tissue. Similar doses of these isotopic fatty acids were administered in both studies.

6.6 Study Limitations

The major shortcoming in our studies and other studies investigating *in vivo* disparities in fibre type functional, metabolic and structural characteristics is the lack of muscle groups with pure fibre type make up. Individual muscles contain different fibre types that include hybrid fibres (the coexistence of different MHC isoforms in a single fibre) to meet the specific demands of the specific muscle. Therefore observations in individual muscles may not necessarily be attributed to specific fibre types. In addition there were limitations related to the quantification of the labelled metabolites. Labelled standards such as $^{13}C_{18}$-20:3n-6, $^{13}C_{18}$-20:4n-6, $^{2}H_{5}$ 20:5n-3 and $^{2}H_{5}$ 22:6n-3 which match *in vivo* metabolites of the labelled n-6 and n-3 precursors are not available. Therefore the calibration curves for the labelled metabolites were made using unlabelled standards, supported by previous work (Lin, Pawlosky, and Salem, Jr., 2005). Responses for 20:3n-6 and 20:5n-3 are slightly different than that of 20:4n-6 and 22:6n-3, respectively, and those of labelled FAMEs are different than unlabelled FAMEs. It is therefore likely that n-6 metabolite enrichments reported in this study are not entirely accurate. Finally, despite the markedly reduced FAME fragmentation under internal isobutane PCI, fragmentation increases as the degree of polyunsaturation increases. The reason for this is that the ionization of these HUFAs requires much lower energies than can be sustained by more unsaturated FAMEs. In particular, fragmentation dramatically increases in fatty acids with >3 carbon-carbon, double bonds. Therefore, some HUFAs such as 20:4n-6, 20:5n-3 and 22:6n-3 must be quantified by high mass fragments rather than parent ions. Further methodological developments that result in higher percentages of HUFA parent ions are desirable to improve sensitivity.

6.7 Future Directions

Long term tracer studies have shown that muscle is labelled rapidly with n-3 and n-6 metabolites (22:6n-3 and 20:4n-6) by the first day and eventually becomes the largest pool of these metabolites partially due to a large relative tissue mass (Lin and Salem, Jr., 2007). According to these findings, future studies on uptake, incorporation and maintenance of AA and DHA in specific muscle types should be explored in longer duration studies and with administration of the preformed labelled AA and DHA rather than their corresponding precursors. The results from this study can enhance and extend our current understanding of the fibre type-specific handling of longer chain PUFAs and it will be the first step towards elucidating potential fibre type specific requirements for AA and DHA.

The β-oxidation rates of the isotopic labelled 18:2n-6 and 22:6n-3 are dramatically reduced in the n-6 and n-3 deficient rats, respectively, compared to control rats (Cunnane and Anderson, 1997a; Waki et al., 2004). These findings imply a remarkable increase in the retention of labelled fatty acids in the whole body compared with animals provided with PUFA adequate diets. Therefore a second potential future project is experimentation on n-6 and n-3 deficient rats which are perhaps better candidates for tracking isotopic PUFAs in the specific muscle types.

With the new advances in the GC-MS quadrupole ion trap analysing capability, there is a growing interest in using hybrid configuration as compared to those of internal and external. Hybrid configuration is a new ionization technique specific to quadrupole ion trap GC-MS systems which combines the valuable features of external and internal ionization with removal of the critical issues for both. As of yet no study has attempted to use hybrid configuration in measuring stable isotopic fatty acids. Application of the hybrid configuration in ionizing FAMEs

appears to be a promising alternative for the current internal PCI method. These methodologies could also be utilized in human studies.

6.8 Conclusions

To date this was the first attempt to systematically compare PUFA uptake, distribution and metabolism among various skeletal muscle types with different fibre types after administration of an acute, single oral bolus of labelled n-6 and n-3 precursors. Using a battery of tracer studies it was revealed that soleus muscle (high type I fibres in rats), was labelled with significantly higher concentrations of uniformly labelled carbon 13-18:2n-6, deuterium labelled 18:3n-3 as compared with those in red gastrocnemius and white gastrocnemius which were similar. Similar rank order was also observed for carbon-13 labelled n-6 metabolites derived from uniformly labelled carbon-13-18:2n-6. The close agreement between the results from tracer studies with those from comparison of the endogenous pool of PUFAs in the examined muscle types demonstrate that muscle type differences in PUFA handling is important and PUFA requirements may differ between muscle types, possibly due to functional and/or structural diversity among different fibre types. Finally the PCI quadrupole ion trap GC/MS technique using isobutane as reagent gas is useful for tracer studies in quantitatively small samples. This technique offers the distinct advantages of simple derivitization of fatty acid and low maintenance over negative chemical ionization while it still has a comparable limit of detection.

Table 5. Concentration of fatty acids in soleus, red gastrocnemius and white gastrocnemius

Fatty acids	Heart	Soleus	Red Gastrocnemius	White Gastrocnemius
		Concentration (μmol/g of tissue)		
10:0	n.d.	0.19 ± 0.06	n.d.	n.d.
12:0	0.04 ± 0.01 ^{b}	0.65 ± 0.15 ^{a}	0.01 ± 0.01 ^{b}	0.03 ± 0.02 ^{b}
14:0	0.30 ± 0.01 ^{b}	1.05 ± 0.19 ^{a}	0.20 ± 0.03 ^{b}	0.24 ± 0.05 ^{b}
16:0	7.38 ± 0.54 ^{ab}	8.13 ± 0.71 ^{a}	5.51 ± 0.38 ^{b}	6.23 ± 0.26 ^{b}
16:0 dma	0.08 ± 0.00 ^{a}	0.21 ± 0.07 ^{ab}	0.32 ± 0.08 ^{b}	0.18 ±.0.04 ^{ab}
18:0	10.92 ± 0.22 ^{c}	5.68 ± 0.19 ^{a}	5.04 ± 0.30 ^{a}	3.26 ± 0.16 ^{b}
18:0 dma	0.12 ± 0.02 ^{a}	0.02 ± 0.00 ^{b}	0.08 ± 0.02 ^{ab}	0.05 ± 0.01 ^{ab}
20:0	0.14 ± 0.01 ^{a}	0.06 ± 0.01 ^{b}	0.03 ± 0.01 ^{c}	0.02 ± 0.01 ^{d}
22:0	0.10 ± 0.00 ^{a}	0.06 ± 0.01 ^{b}	0.04 ± 0.01 ^{c}	0.02 ± 0.01 ^{d}
24:0	0.08 ± 0.00 ^{a}	0.06 ± 0.01 ^{b}	0.05 ± 0.01 ^{b}	0.03 ± 0.01 ^{c}
Total SFA	19.17 ± 0.72 ^{a}	16.11 ± 1.39 ^{a}	11.29 ± 0.82 ^{b}	10.06 ± 0.55 ^{b}
14:1	0.10 ± 0.01 ^{a}	0.05 ±0.02 ^{a}	0.07 ± 0.01 ^{a}	0.09 ± 0.02 ^{a}
16:1	0.11 ± 0.02 ^{b}	0.73 ± 0.14 ^{a}	0.09 ± 0.01 ^{b}	0.12 ±.0.02 ^{b}
18:1n-9	3.39 ± 0.78 ^{ab}	5.54 ± 0.79 ^{a}	1.77 ± 0.16 ^{b}	1.80 ± 0.16 ^{b}
18:1n-7	1.68 ± 0.17 ^{a}	1.10 ± 0.07 ^{c}	0.79 ± 0.07 ^{b}	0.72 ± 0.03 ^{b}
Total MUFA	5.45 ± 0.99 ^{ab}	7.59 ± 1.04 ^{a}	2.85 ± 0.28 ^{b}	2.80 ± 0.24 ^{b}
18:2n-6	7.93 ± 0.82 ^{ab}	11.15 ± 1.37 ^{a}	5.87 ± 0.51 ^{b}	5.09 ± 0.29 ^{b}
18:3n-6	0.01 ± 0.00 ^{b}	0.06 ± 0.01 ^{a}	0.03 ± 0.01 ^{b}	0.02 ± 0.01 ^{b}
20:2n-6	0.17 ± 0.01 ^{a}	0.18 ± 0.01 ^{a}	0.15 ± 0.01 ^{a}	0.15 ± 0.01 ^{a}
20:3n-6	0.17 ± 0.01 ^{a}	0.23 ± 0.01 ^{a}	0.20 ± 0.16 ^{a}	0.22 ± 0.01 ^{a}
20:4n-6	8.65 ± 0.74 ^{a}	4.27 ± 0.18 ^{b}	3.94 ± 0.30 ^{b}	3.54 ± 0.17 ^{b}
22:4n-6	0.66 ± 0.06 ^{a}	0.40 ± 0.01 ^{b}	0.35 ± 0.03 ^{b}	0.37 ± 0.02 ^{b}
22:5n-6	0.71 ± 0.03 ^{a}	0.34 ± 0.01 ^{b}	0.35 ± 0.02 ^{b}	0.27 ± 0.01 ^{c}
Total n-6 PUFA	18.31 ± 1.66 ^{a}	16.63 ± 1.62 ^{a}	10.88 ± 0.89 ^{b}	9.66 ± 0.50 ^{b}
18:3n-3	0.19 ± 0.02 ^{a}	0.61 ± 0.11 ^{a}	0.10 ± 0.01 ^{b}	0.11 ± 0.01 ^{b}
20:5n-3	0.05 ± 0.00 ^{a}	0.07 ±0.01 ^{bc}	0.06 ± 0.01 ^{ab}	0.09 ± 0.01 ^{cd}
22:5n-3	1.23 ± 0.10 ^{a}	0.78 ± 0.03 ^{b}	0.81 ± 0.07 ^{b}	0.63 ± 0.04 ^{b}
22:6n-3	3.77 ± 0.26 ^{a}	2.30 ± 0.06 ^{b}	2.38 ± 0.18 ^{b}	1.32 ± 0.07 ^{c}
Total n-3 PUFA	5.24 ± 0.38 ^{a}	3.76 ± 0.21 ^{b}	3.35 ± 0.26 ^{b}	2.14 ± 0.13 ^{c}
Total PUFA	23.54 ± 2.03 ^{a}	20.38 ± 1.83 ^{a}	14.24 ± 1.15 ^{b}	11.80 ± 0.64 ^{b}
Total HUFA	15.23 ± 1.19 ^{a}	8.39 ± 0.33 ^{b}	8.09 ± 0.61 ^{b}	6.43 ± 0.32 ^{b}
N-6/N-3	3.81 ± 0.27 ^{a}	4.43 ± 0.32 ^{b}	3.25 ± 0.87 ^{a}	4.51 ± 0.54 ^{b}
Total fatty acids	48.15 ± 3.71 ^{a}	44.08 ± 4.27 ^{a}	28.37 ± 2.25 ^{b}	24.67 ± 1.43 ^{b}

Values are means ± SEM; n = 8. Values in a row not sharing a roman superscript are significantly different at $P < 0.05$ by Tukey's honestly significantly difference test after a significant F-value ($P < 0.05$) by one way ANOVA. SFA, saturated fatty acids; MUFA, monounsaturated fatty acids; PUFA, polyunsaturated fatty acids

Table 6. Molar percentage of fatty acids in soleus, red gastrocnemius and white gastrocnemius**.**

Fatty acids	Heart	Soleus	Red Gastrocnemius	White Gastrocnemius
		(Molar % of total fatty acids)		
10:0	n.d.	0.39 ± 0.11	n.d.	n.d.
12:0	0.09 ± 0.01 [a]	1.37 ± 0.25 [b]	0.04 ± 0.01 [a]	0.21 ± 0.06 [a]
14:0	0.64 ± 0.05 [a]	2.30 ± 0.28 [b]	0.75 ± 0.13 [a]	0.98 ± 0.19 [a]
16:0	15.36 ± 0.20 [a]	18.46 ± 0.23 [b]	19.48 ± 0.39 [b]	25.16 ± 0.19 [c]
16:0 dma	0.17 ± 0.02 [a]	0.59 ± 0.18 [a]	1.02 ± 0.22 [b]	0.73 ± 0.16 [a]
18:0	23.10 ± 1.54 [a]	13.36 ± 0.99 [b]	17.91 ± 0.56 [c]	13.37 ± 0.33 [b]
18:0 dma	0.24 ± 0.02 [a]	n.d.	0.27 ±.0.07 [b]	0.21 ± 0.14 [b]
20:0	0.31 ± 0.00 [a]	0.17 ± 0.02 [b]	0.13 ± 0.02 [b]	0.06 ± 0.01 [c]
22:0	0.23 ± 0.02 [a]	0.13 ± 0.01 [b]	0.12 ± 0.01 [b]	0.07 ± 0.01 [c]
24:0	0.17 ± 0.02 [ab]	0.13 ± 0.01 [a]	0.18 ± 0.02 [b]	0.12 ± 0.01 [a]
Total SFA	40.28 ± 1.71 [ab]	36.64 ± 0.66 [a]	40.10 ± 0.88 [ab]	41.38 ± 0.62 [b]
14:1	0.20 ± 0.02 [a]	0.13 ± 0.05 [a]	0.25 ±0.06 [a]	0.21 ± 0.07 [a]
16:1	0.22 ± 0.02 [a]	1.58 ± 0.20 [b]	0.30 ± 0.06 [a]	0.50 ± 0.04 [a]
18:1n-9	6.73 ± 1.11 [a]	12.25 ± 0.78 [b]	6.23 ± 0.27 [a]	7.23 ± 1.00 [a]
18:1n-7	3.47 ± 0.10 [a]	2.25 ± 0.10 [b]	2.75 ± 0.07 [bc]	2.90 ± 0.51 [c]
20:1n-9	0.13 ± 0.13 [a]	0.18 ± 0.02 [a]	0.14 ± 0.02 [a]	0.13 ± 0.01 [a]
Total MUFA	10.96 ± 1.22 [a]	16.91 ± 0.83 [b]	10.02 ± 0.35 [a]	11.44 ± 0.43 [a]
18:2n-6	16.36 ± 0.60 [a]	24.86 ± 1.02 [b]	20.53 ± 0.52 [c]	20.37 ± 0.40 [c]
18:3n-6	0.02 ± 0.00 [a]	0.13 ± 0.02 [b]	0.09 ± 0.01 [c]	0.07 ± 0.01 [c]
20:2n-6	0.35 ± 0.01 [a]	0.41 ± 0.01 [b]	0.54 ± 0.01 [c]	0.59 ± 0.02 [d]
20:3n-6	0.35 ± 0.01 [a]	0.52 ± 0.02 [b]	0.70 ± 0.01 [c]	0.99 ± 0.09 [d]
20:4n-6	17.79 ± 0.21 [a]	10.02 ± 0.71 [b]	13.85 ± 0.14 [c]	14.35 ± 0.54 [c]
22:4n-6	1.36 ± 0.02 [a]	0.94 ± 0.06 [b]	1.26 ± 0.08 [a]	1.50 ± 0.05 [a]
22:5n-6	1.48 ± 0.05 [a]	0.80 ± 0.08 [b]	1.24 ± 0.05 [ac]	1.10 ± 0.07 [c]
Total n-6 PUFA	37.87 ± 0.77 [a]	37.69 ± 0.36 [a]	38.20 ± 0.59 [a]	38.54 ± 0.60 [a]
18:3n-3	0.39 ± 0.02 [a]	1.33 ± 0.13 [b]	0.36 ± 0.02 [a]	0.44 ± 0.04 [a]
20:5n-3	0.10 ± 0.00 [a]	0.16 ± 0.01 [b]	0.23 ± 0.01 [c]	0.33 ± 0.01 [d]
22:5n-3	2.56 ± 0.06 [a]	1.83 ± 0.14 [b]	2.83 ± 0.06 [a]	2.46 ± 0.10 [a]
22:6n-3	7.84 ± 0.18 [a]	5.43 ± 0.44 [b]	8.38 ± 0.10 [a]	5.34 ± 0.22 [b]
Total n-3 PUFA	10.89 ± 0.21 [a]	8.75 ± 0.44 [b]	11.83 ± 0.15 [a]	8.45 ± 0.31 [b]
Total PUFA	48.76 ± 0.61 [ab]	46.45 ± 0.49 [a]	50.03 ± 0.67 [b]	46.99 ± 0.86 [a]
Total HUFA	31.62 ± 0.18 [a]	19.70 ± 1.42 [b]	28.48 ± 0.27 [ac]	25.37 ± 0.90 [c]
N-6/N-3	3.50 ± 0.15 [a]	4.38 ± 0.24 [b]	3.23 ± 0.05 [a]	4.60 ± 0.13 [b]

Values are means ± SEM; n = 8. Values in a row not sharing a roman superscript are significantly different at $P < 0.05$ by Tukey's honestly significantly difference test after a significant F-value ($P < 0.05$) by one-way ANOVA. SFA, saturated fatty acids; MUFA, monounsaturated fatty acids; PUFA, polyunsaturated fatty acids

Table 7. Accumulation of labelled 18:2n-6, 20:3n-6 and 20:4n-6 in various muscle types as a percentage of total precursor dose.

		18:2n-6			20:3n-6		20:4n-6	
	Wt.(g)	$^{13}C_{18}$-EE	$^{13}C_{18}$-NEFA	$^{2}H_{5}$-EE	$^{13}C_{18}$-EE	$^{13}C_{18}$-NEFA	$^{13}C_{18}$-EE	$^{13}C_{18}$-NEFA
Soleus	0.098	0.021	0.025	0.002	0.0002	0.0003	0.002	0.001
Red G.	0.324	0.022	0.028	0.005	0.0002	0.0002	n.d.	n.d.
White G.	0.275	0.013	0.017	0.002	n.d.	n.d.	n.d.	n.d.

Values are expressed as mean, n=4. $^{13}C_{18}$-EE, ethyl ester form of ^{13}C-labelled fatty acid; $^{13}C_{18}$-NEFA, nonesterified fatty acid form of ^{13}C-labelled fatty acid; $^{2}H_{5}$-EE; ethyl ester form of ^{2}H-labelled fatty acid. Red G, red gastrocnemius; White G, white gastrocnemius; n.d., not detected

Table 8. Comparison of net accumulation and enrichment of major n-6 metabolites in rat skeletal muscles 8 h after dosing with labelled 18:2n-6.

Fatty acid	Isotope	Soleus		Red Gastrocnemius	
		nmol/g	% endogenous pool	nmol/g	% endogenous pool
20:3n-6	$^{13}C_{18}$ EE	1.21 ± 0.29	0.53 ± 0.13	0.26 ± 0.07	0.13 ± 0.03
	$^{13}C_{18}$ FFA	1.65 ± 0.14	0.72 ± 0.06	0.32 ± 0.03	0.16 ± 0.01
20:4n-6	$^{13}C_{18}$ EE	7.82 ± 0.49	0.18 ± 0.01	n.d.	n.d.
	$^{13}C_{18}$ FFA	8.65 ± 0.3	0.20 ± 0.01	n.d.	n.d.

Values are means ± SEM for 4 rats in units of nmol / g of tissue. Tr; trace amount of the metabolite was detected 8 h after dosing with the labelled 18:2n-6; n.d., not detected. $^{13}C_{18}$ EE, ethyl ester form of uniformly labelled carbon 13; $^{13}C_{18}$ NEFA, nonesterified fatty acid form of the uniformly labelled carbon 13.

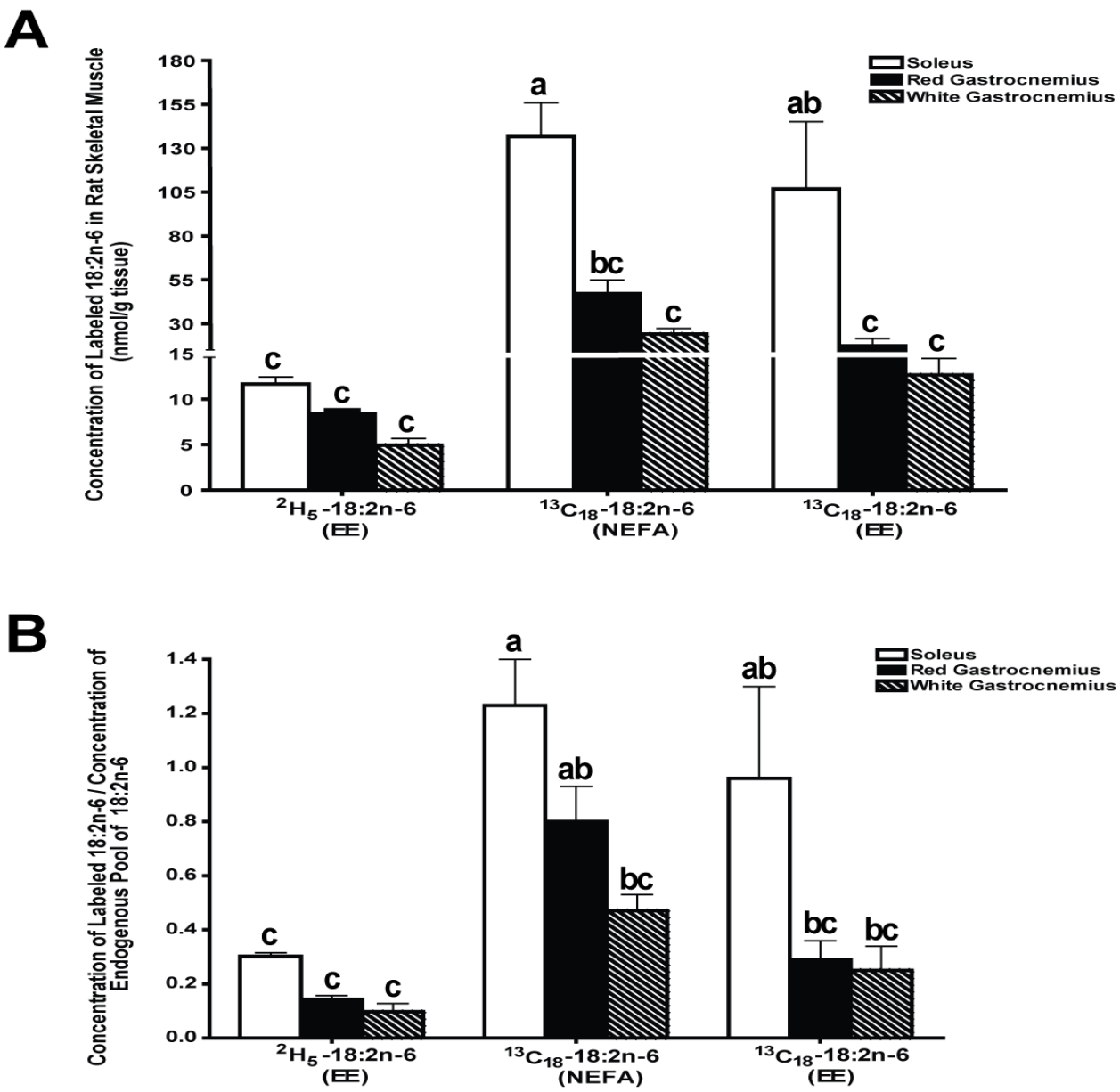

Figure 6. Comparison of isotope-labelled linoleate in soleus, red gastrocnemius and white gastrocnemius muscles. Data are expressed as means ± SEM at 8 h after oral dosing; n = 4. A) Net accumulation of the labelled linoleate in nmol/g of muscle B) Muscle enrichment with labelled linoleate expressed as percentage of endogenous pool of linoleate. Two-way ANOVA analysis of the means revealed a significant interaction for the net accumulation and enrichment data (P = 0.03). Individual means were compared using Tukey's honestly significantly difference test across various muscle types. Significant differences are denoted by different lowercase letters. $P < 0.05$.

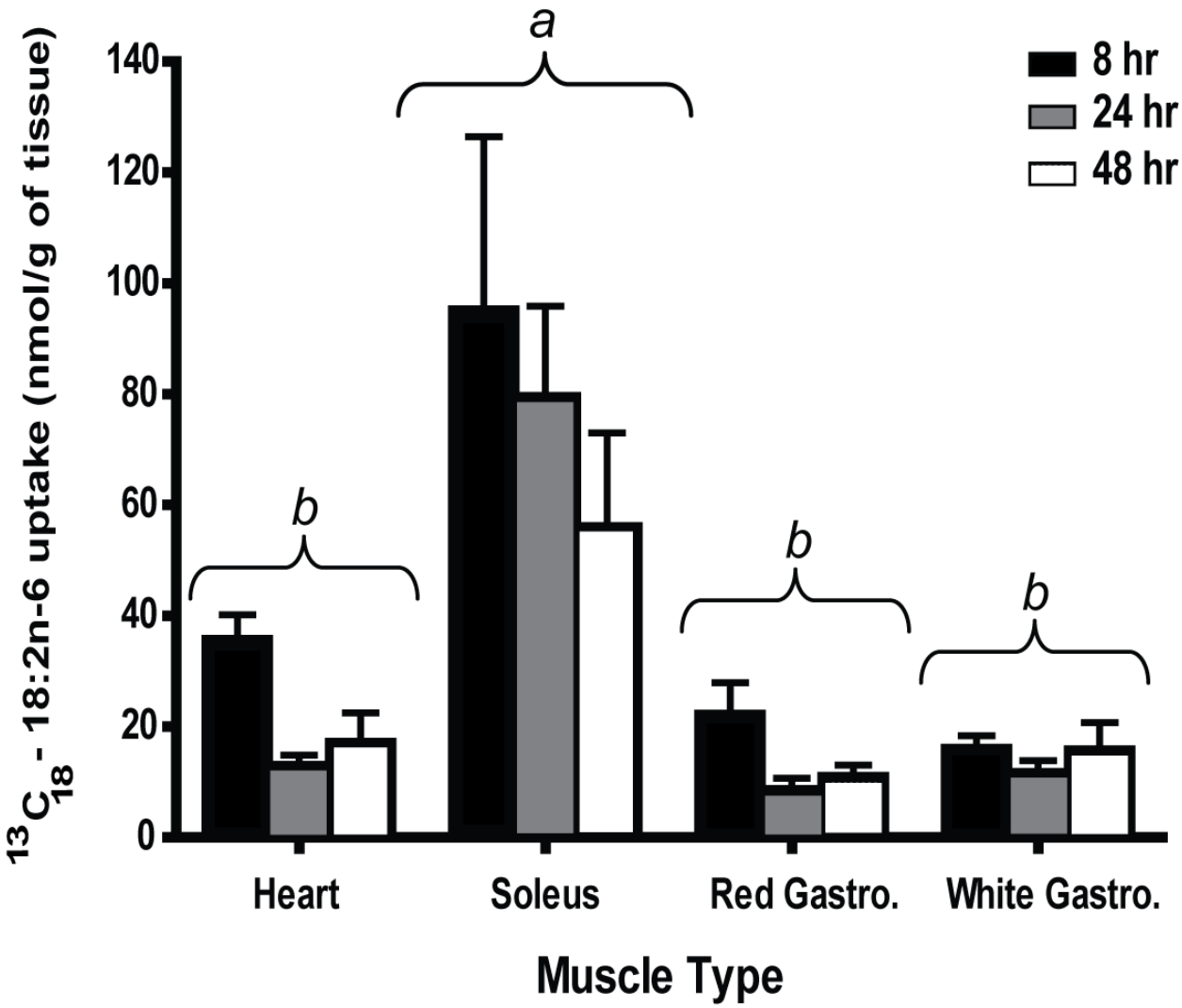

Figure 7. Time-course plots of the concentrations (nmol/g tissue) of $^{13}C_{18}$-18:2n-6 in various muscle types over 2 days period following a single oral dosing. Values are mean ± SEM, n=5. Two-way ANOVA analysis of the means revealed no interaction ($P = 0.72$), and no main effect of time ($P = 0.10$). A significant main effect for muscle type was detected ($P < 0.0001$). Individual means were compared using Tukey's honestly significantly difference test across various muscle types. Significantly different muscle types are denoted by different lowercase letters. $P < 0.05$. Gastro, gastrocnemius muscle.

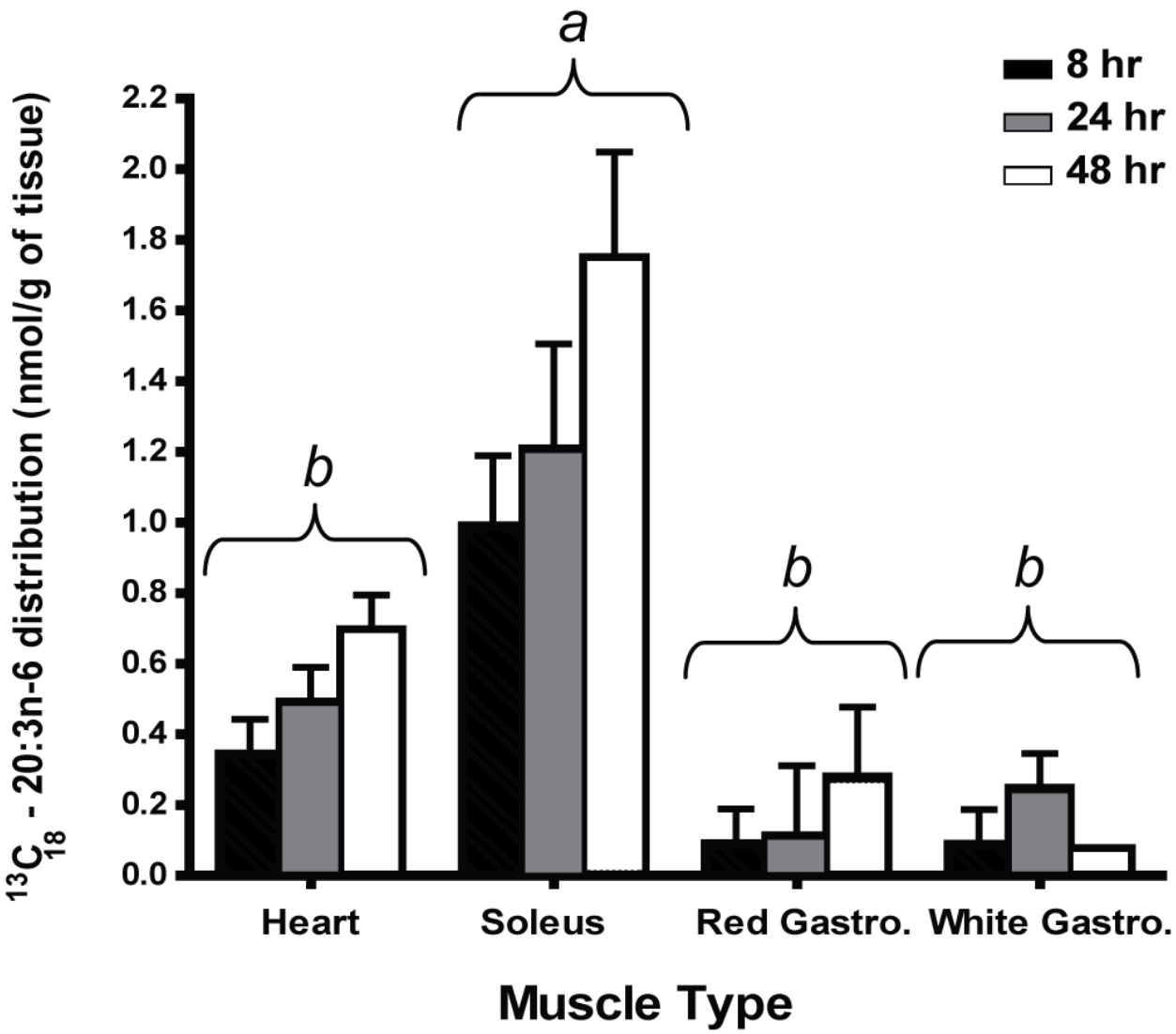

Figure 8. Time-course plots of the concentrations (nmol/g tissue) of $^{13}C_{18}$-20:3n-6 in various muscle types over 2 days following a single oral dosing. Values are mean ± SEM, n=5. Two-way ANOVA analysis of the means revealed no interaction ($P = 0.37$) and no main effect for time ($P = 0.06$). A significant main effect for muscle type was detected ($P < 0.0001$). Individual means were compared using Tukey's honestly significantly difference test across various muscle types. Significantly different muscle types are denoted by different lowercase letters. $P < 0.05$. Gastro, gastrocnemius muscle.

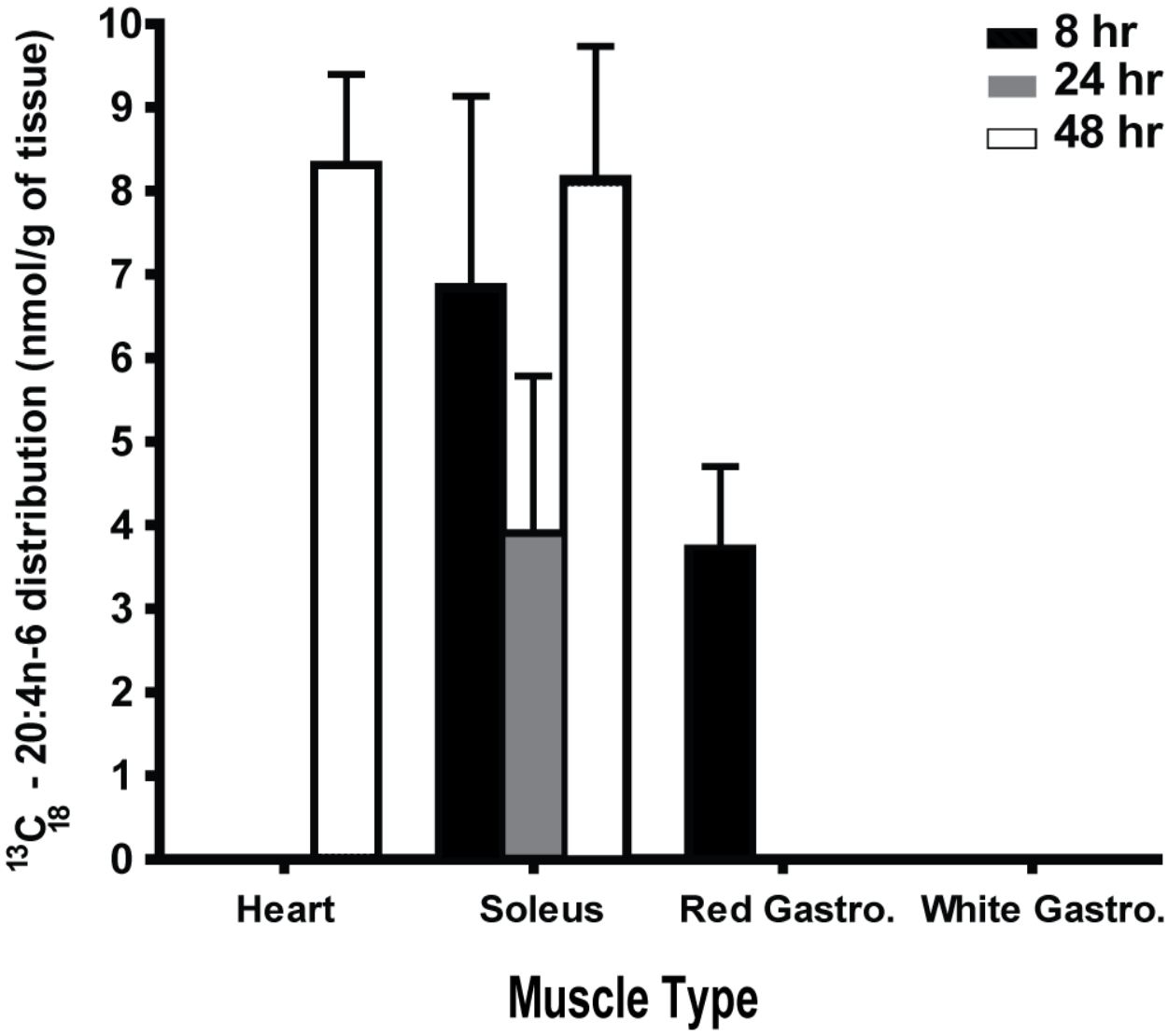

Figure 9. Time-course plots of the concentrations (nmol/g tissue) of $^{13}C_{18}$-20:4n-6 in various muscle types over 2 days following a single oral dosing. Values are mean ± SEM, n=5. Two-way ANOVA analysis of the means revealed a significant interaction ($P < 0.0001$). However, there were no differences between individual means by Tukey's honestly significant difference test. Gastro, gastrocnemius muscle.

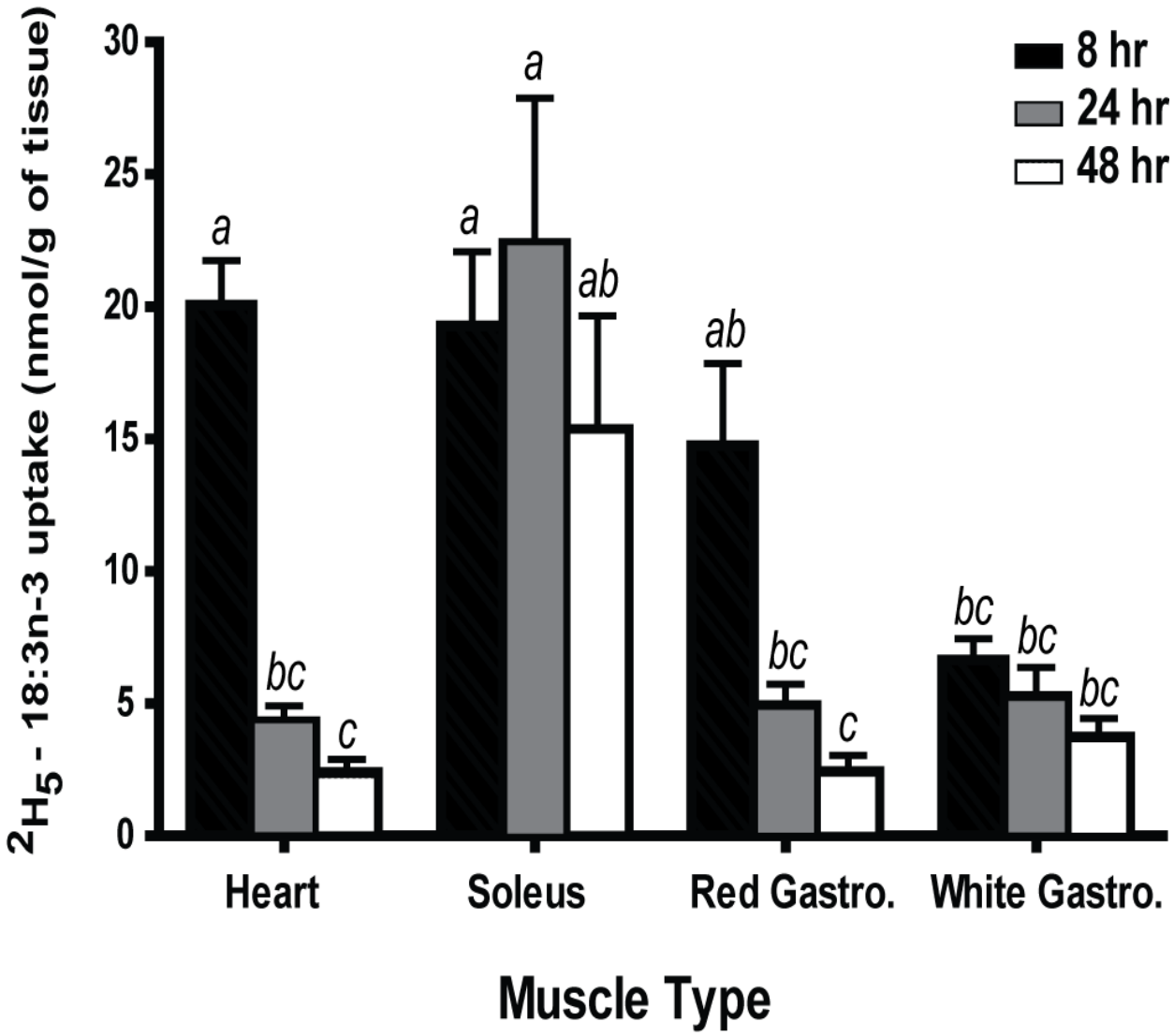

Figure 10. Time-course plots of the concentrations (nmol/g tissue) of $^2H_5$-18:3n-3 in various muscle types over 2 days following a single oral dosing. Values are mean ± SEM, n=5. Two-way ANOVA analysis of the means revealed a significant interaction (P = 0.006). Tukey's honestly significantly difference test was used to determine the significant differences in concentration of $^2H_5$-18:3n-3 among various muscle types at different time points. Graph bars not sharing the same lowercase letter are significantly different. $P < 0.05$. Gastro, gastrocnemius muscle.

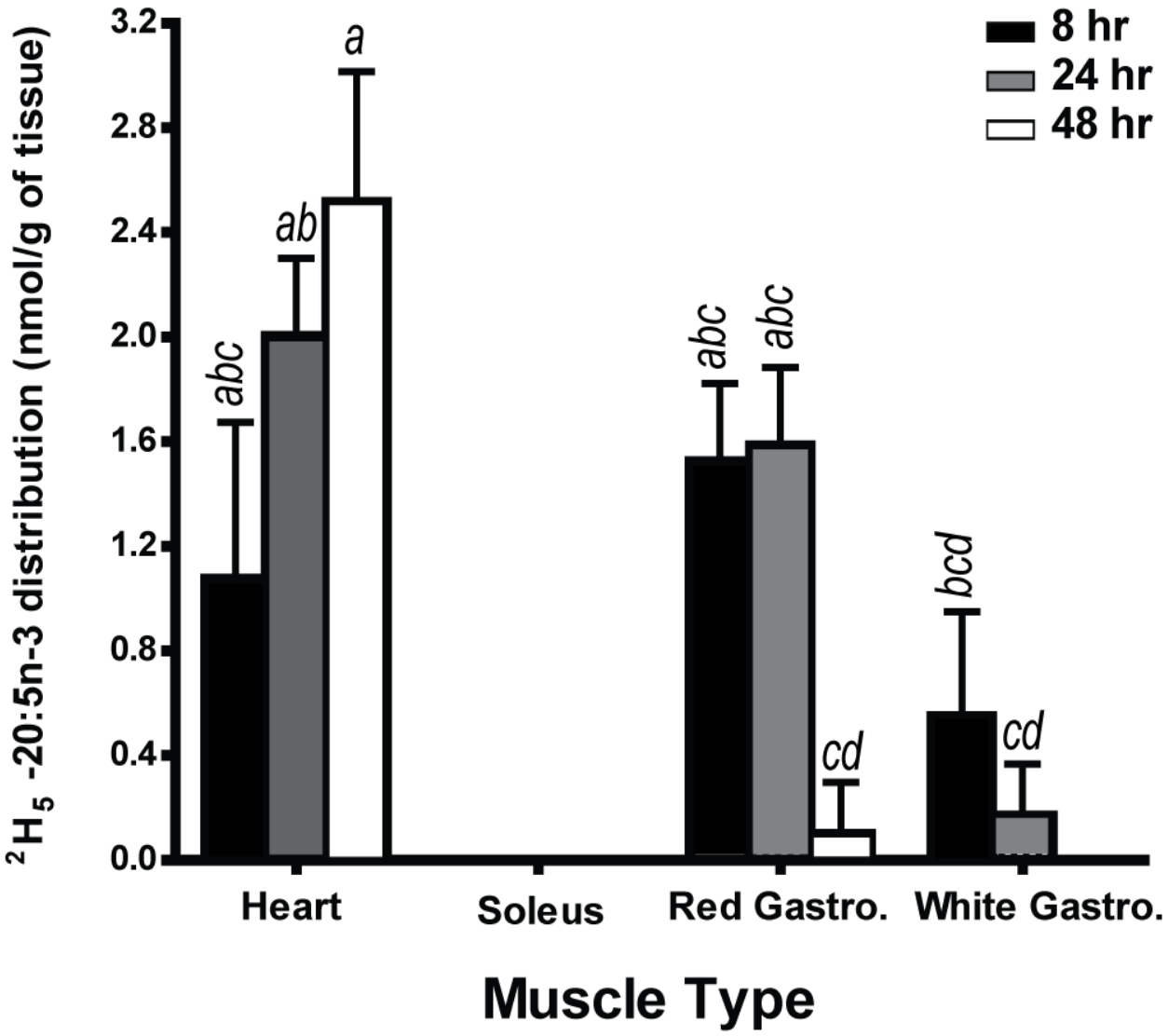

Figure 11. Time-course plots of the concentrations (nmol/g tissue) of $^2H_5$-20:5n-3 in various muscle types over 2 days following a single oral dosing. Values are mean ± SEM, n=5. Two-way ANOVA analysis of the means revealed a significant interaction (P = 0.001). Tukey's honestly significant difference test was used to determine the significant differences in concentration of $^2H_5$-20:5n-3 among various muscle types at different time points. Graph bars not sharing the same lowercase letter are significantly different. $P < 0.05$. Gastro, gastrocnemius muscle.

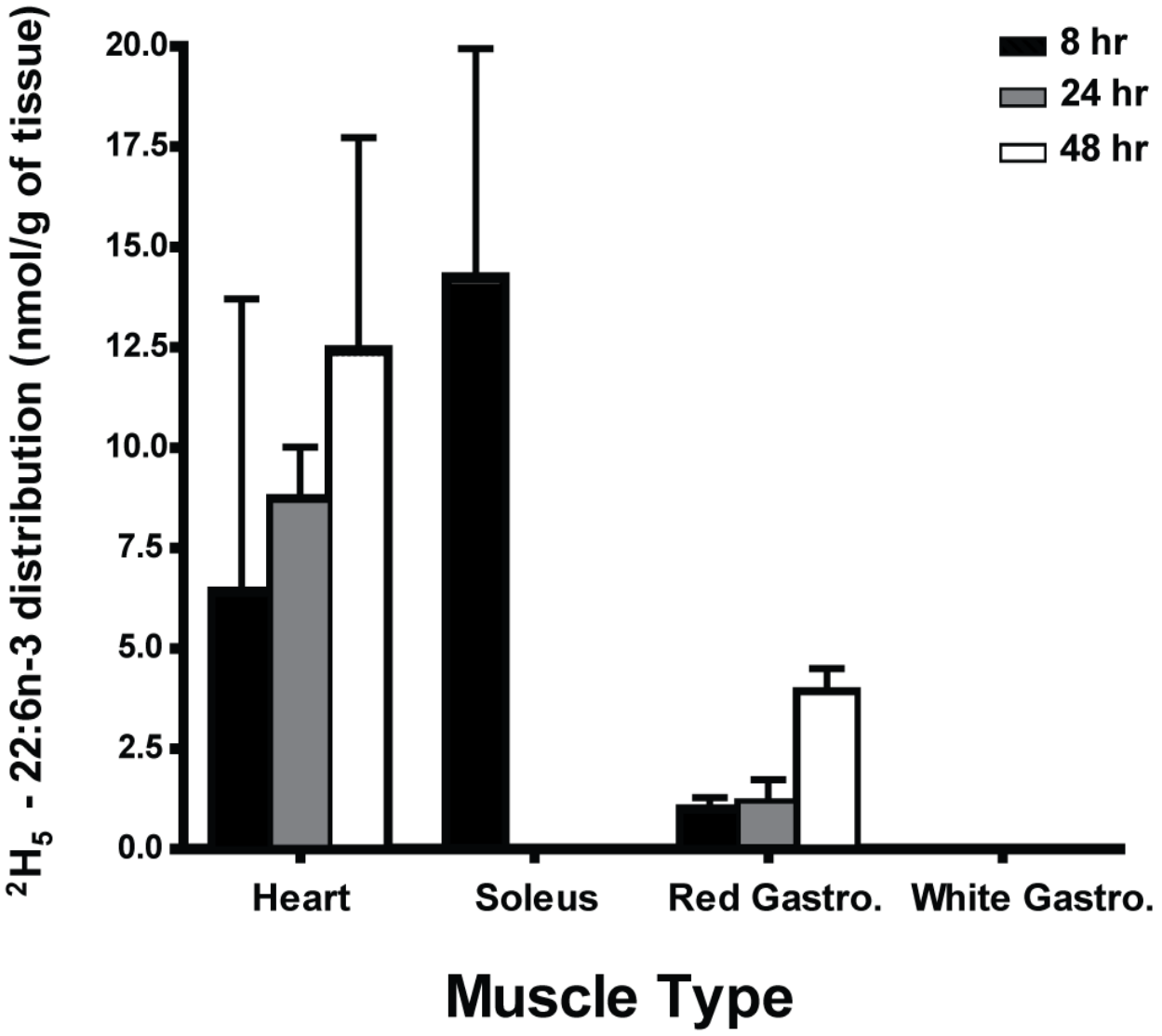

Figure 12. Time-course plots of the concentrations (nmol/g tissue) of $^2H_5$-22:6n-3 in various muscle types over 2 days following a single oral dosing. Values are mean ± SEM, n=5. Two-way ANOVA analysis of the means revealed a significant interaction ($P = 0.04$). However, there were no differences between individual means by Tukey's honestly significant difference test. $P < 0.05$. Gastro, gastrocnemius muscle.

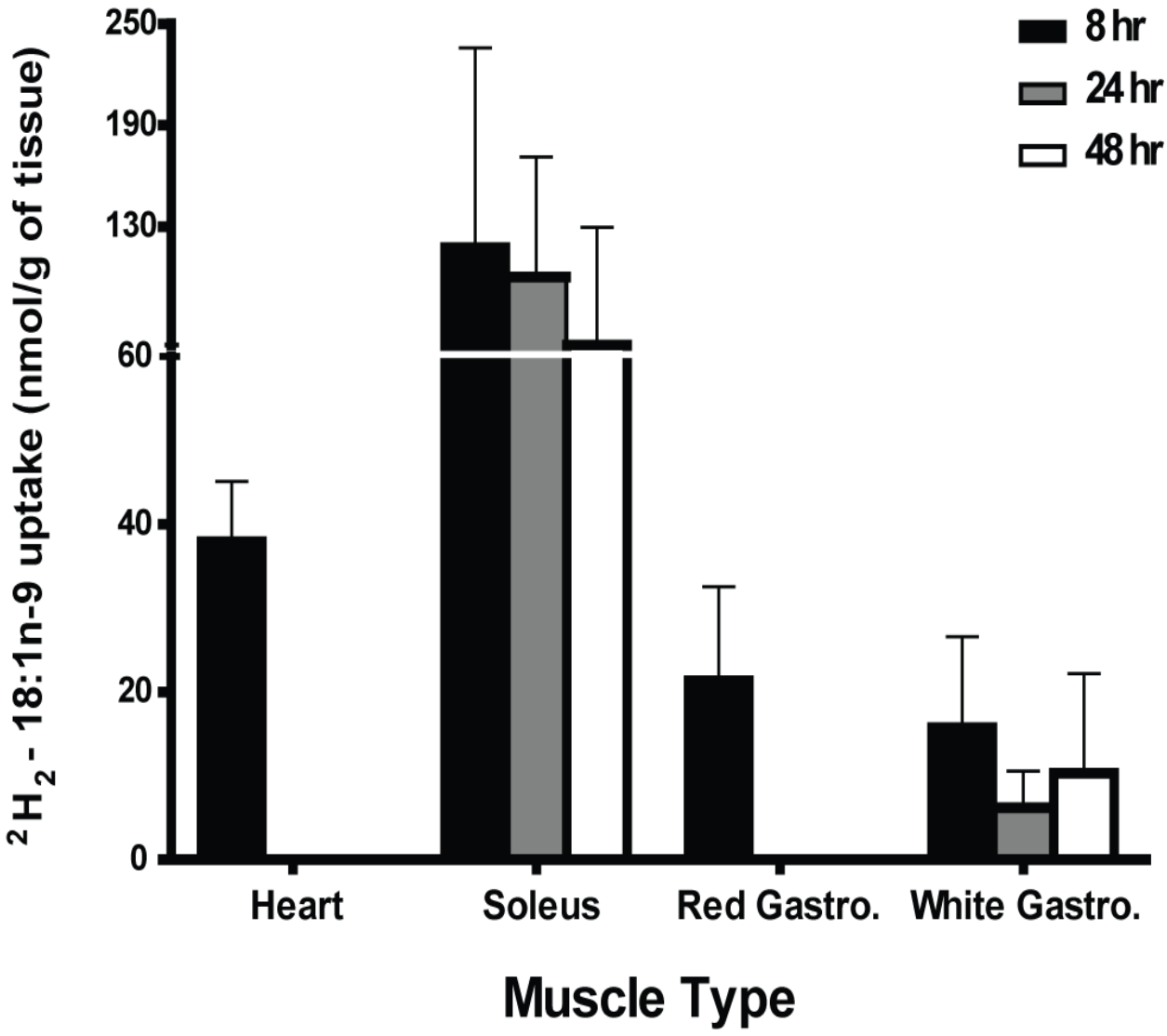

Figure 13. Time-course plots of the concentrations (nmol/g tissue) of $^2H_2$-18:1n-9 in various muscle types over 2 days following a single oral dosing. Values are mean ± SEM, n=5. Two-way ANOVA analysis of the means revealed no interaction (P = 0.99) and there was also no main effects for time (P = 0.62) and muscle type (P = 0.07). Gastro, gastrocnemius muscle.

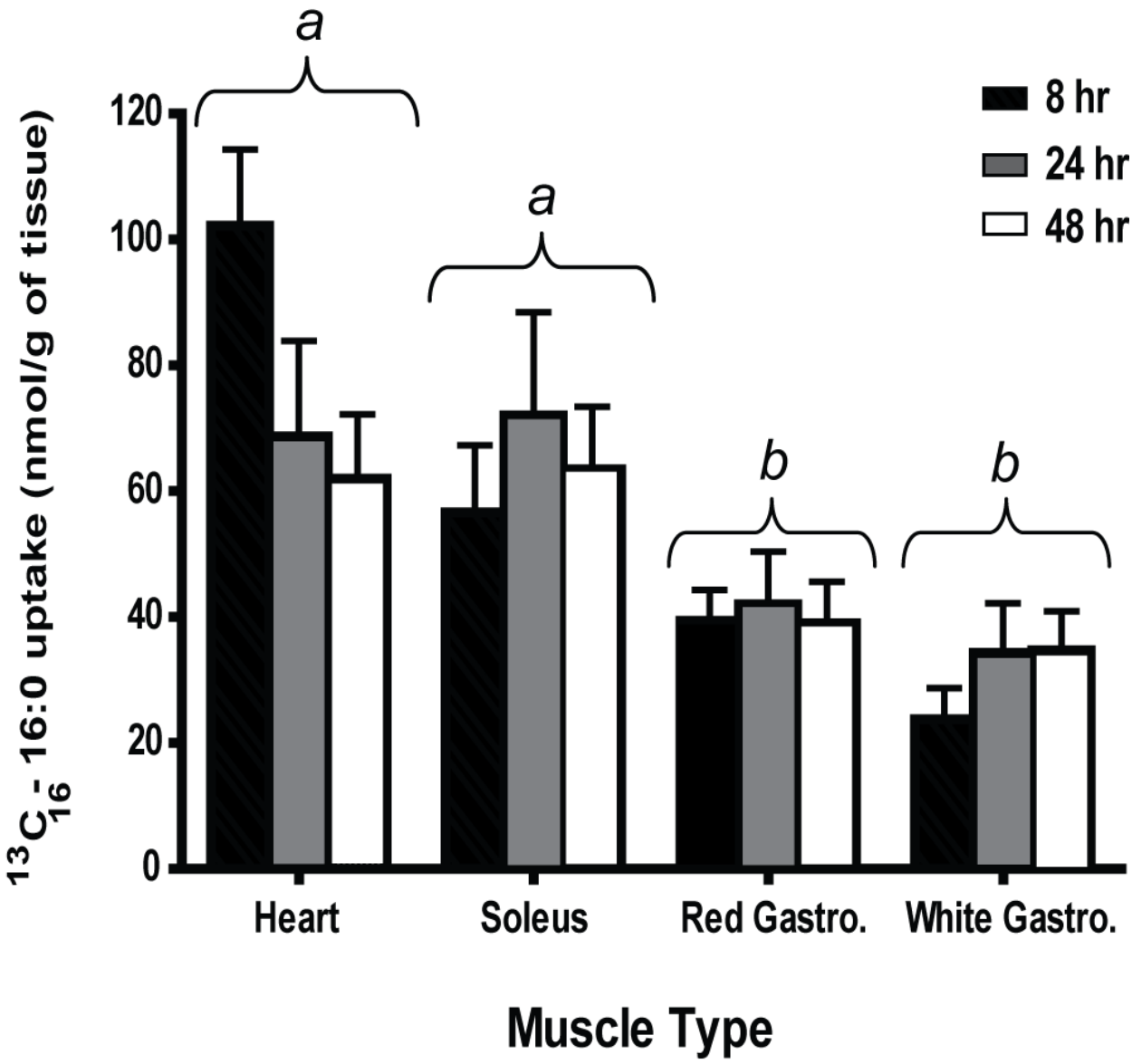

Figure 14. Time-course plots of the concentrations (nmol/g tissue) of $^{13}C_{16}$-16:0 in various muscle types over 2 days following a single oral dosing. Values are mean ± SEM, n=5. Two-way ANOVA analysis of the means revealed no interaction ($P = 0.13$), and no main effect of time ($P = 0.70$). However, there was a significant main effect for muscle type ($P < 0.0001$). Individual means were compared using Tukey's honestly significantly difference test across various muscle types. Significantly different muscle types are denoted by different lowercase letters. $P < 0.05$. Gastro, gastrocnemius muscle.

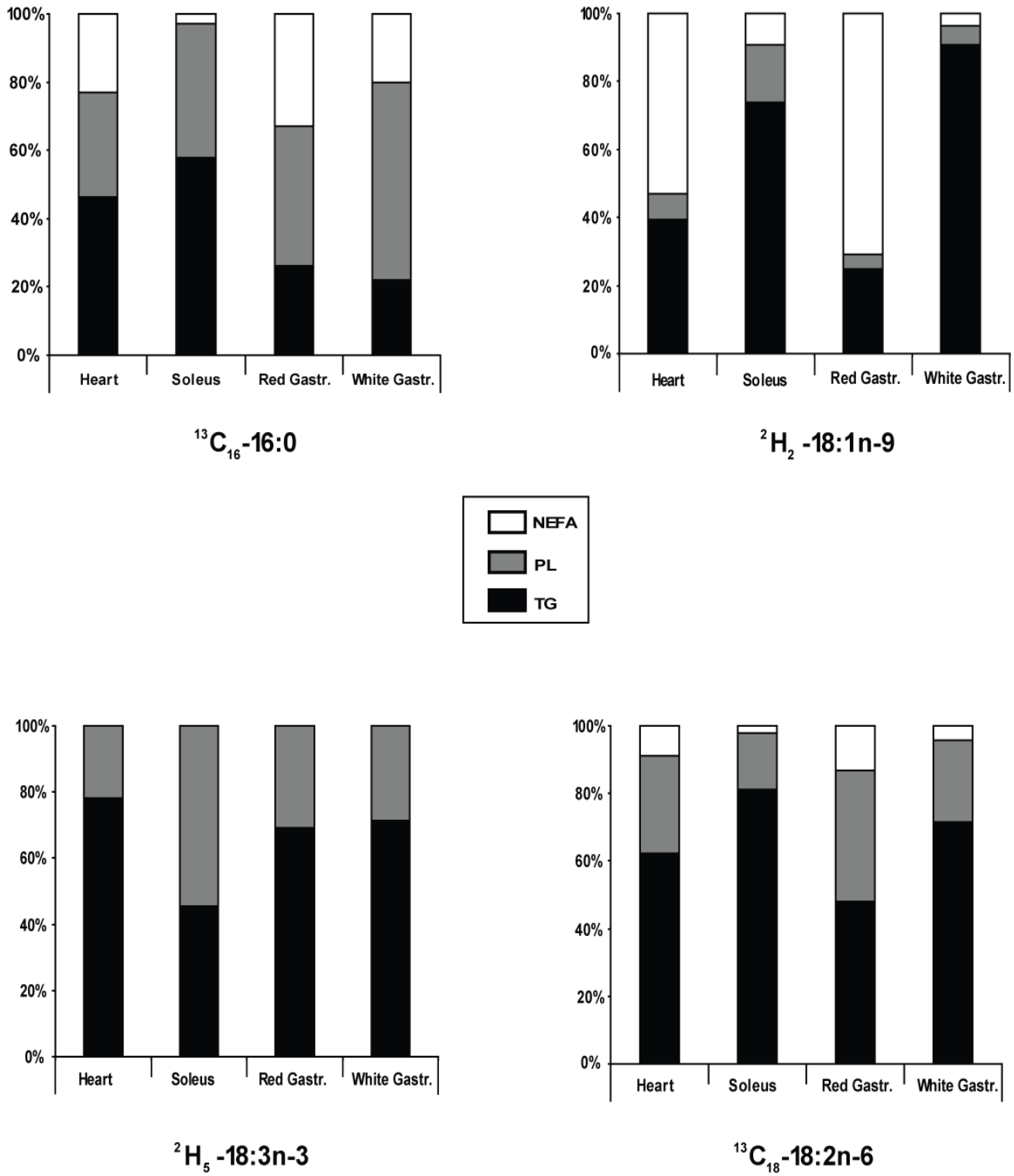

Figure 15. Compartmentalization of $^{13}C_{18}$-18:2n-6, $^{2}H_{5}$-18:3n-3, $^{13}C_{16}$-16:0 and $^{2}H_{2}$-18:1n-9 into TG, PL and NEFA fractions in various muscle types. TG; triglycerols, PL; phospholipids, NEFA: nonesterfied fatty acids**.** Data are mean ± SEM. n=5.

References

Abumrad, N., Coburn, C., & Ibrahimi, A. (1999) Membrane proteins implicated in long-chain fatty acid uptake by mammalian cells: CD36, FATP and FABPm. Biochim.Biophys.Acta 1441: 4-13.

Aigner, S., Gohlsch, B., Hamalainen, N. et al. (1993) Fast myosin heavy chain diversity in skeletal muscles of the rabbit: heavy chain IId, not IIb predominates. Eur.J.Biochem. 211: 367-372.

Andersen, J. L., Schjerling, P., & Saltin, B. (2000) Muscle, genes and athletic performance. Sci Am. 283: 48-55.

Armstrong, R. B. & Laughlin, M. H. (1985) Rat muscle blood flows during high-speed locomotion. J.Appl.Physiol 59: 1322-1328.

Armstrong, R. B. & Phelps, R. O. (1984) Muscle fiber type composition of the rat hindlimb. Am.J.Anat. 171: 259-272.

Ayre, K. J. & Hulbert, A. J. (1996) Effects of changes in dietary fatty acids on isolated skeletal muscle functions in rats. J Appl.Physiol 80: 464-471.

Barker, J. (2000) Mass Spectrometry John Wiley & Sons, New York.

Berberich, D. W., Hail, M. E., Johnson, J. V. et al. (1989) Mass-selection of reactant ions for chemical ionization in quadrupole ion trap and triple quadrupole mass spectrometer. International Journal of Mass Spectrometry and Ion Processes 94.

Bickerton, A. S., Roberts, R., Fielding, B. A. et al. (2007) Preferential uptake of dietary Fatty acids in adipose tissue and muscle in the postprandial period. Diabetes 56: 168-176.

Blackard, W. G., Li, J., Clore, J. N. et al. (1997) Phospholipid fatty acid composition in type I and type II rat muscle. Lipids 32: 193-198.

Bligh, E. G. & Dyer, W. J. (1959) A rapid method of total lipid extraction and purification. Can.J.Biochem.Physiol 37: 911-917.

Bonen, A., Luiken, J. J., Arumugam, Y. et al. (2000) Acute regulation of fatty acid uptake involves the cellular redistribution of fatty acid translocase. J.Biol.Chem. 275: 14501-14508.

Bonen, A., Luiken, J. J., Liu, S. et al. (1998) Palmitate transport and fatty acid transporters in red and white muscles. Am.J.Physiol 275: E471-E478.

Bourre, J. M., Piciotti, M., Dumont, O. et al. (1990) Dietary linoleic acid and polyunsaturated fatty acids in rat brain and other organs. Minimal requirements of linoleic acid. Lipids 25: 465-472.

Burdge, G. C. & Calder, P. C. (2005) Conversion of alpha-linolenic acid to longer-chain polyunsaturated fatty acids in human adults. Reprod.Nutr.Dev. 45: 581-597.

Burdge, G. C. & Wootton, S. A. (2002) Conversion of alpha-linolenic acid to eicosapentaenoic, docosapentaenoic and docosahexaenoic acids in young women. Br.J.Nutr. 88: 411-420.

Burkholder, T. J., Fingado, B., Baron, S. et al. (1994) Relationship between muscle fiber types and sizes and muscle architectural properties in the mouse hindlimb. J.Morphol. 221: 177-190.

Calder, P. C. (2004) n-3 Fatty acids and cardiovascular disease: evidence explained and mechanisms explored. Clin.Sci.(Lond) 107: 1-11.

Carlier, H., Bernard, A., & Caselli, C. (1991) Digestion and absorption of polyunsaturated fatty acids. Reprod.Nutr.Dev. 31: 475-500.

Carlson, S. E. & Neuringer, M. (1999) Polyunsaturated fatty acid status and neurodevelopment: a summary and critical analysis of the literature. Lipids 34: 171-178.

Chabowski, A., Chatham, J. C., Tandon, N. N. et al. (2006) Fatty acid transport and FAT/CD36 are increased in red but not in white skeletal muscle of ZDF rats. Am.J.Physiol Endocrinol.Metab 291: E675-E682.

Chabowski, A., Coort, S. L., Calles-Escandon, J. et al. (2005) The subcellular compartmentation of fatty acid transporters is regulated differently by insulin and by AICAR. FEBS Lett. 579: 2428-2432.

Cho, H. P., Nakamura, M. T., & Clarke, S. D. (1999) Cloning, expression, and nutritional regulation of the mammalian Delta-6 desaturase. J.Biol.Chem. 274: 471-477.

Christensen, M. S., Hoy, C. E., Becker, C. C. et al. (1995) Intestinal absorption and lymphatic transport of eicosapentaenoic (EPA), docosahexaenoic (DHA), and decanoic acids: dependence on intramolecular triacylglycerol structure. Am.J.Clin.Nutr. 61: 56-61.

Christie, W. W. (1989) Gas chromatography and lipids The Oily Press, Glasgow.

Christie, W. W. (2003) Lipid Analysis: Isolation, Separation, Identification and Structural Analysis of Lipids The OIly Press, Bridgwater.

Clarke, S. D. & Jump, D. B. (1994) Dietary polyunsaturated fatty acid regulation of gene transcription. Annu.Rev.Nutr. 14: 83-98.

Coyle, E. F. (1999) Physiological determinants of endurance exercise performance. J.Sci.Med.Sport 2: 181-189.

Cunnane, S. C. & Anderson, M. J. (1997a) Pure linoleate deficiency in the rat: influence on growth, accumulation of n-6 polyunsaturates, and [1-14C]linoleate oxidation. J.Lipid Res. 38: 805-812.

Cunnane, S. C. & Anderson, M. J. (1997b) The majority of dietary linoleate in growing rats is beta-oxidized or stored in visceral fat. J.Nutr. 127: 146-152.

Decker, E. A. (1996) The role of stereospecific saturated fatty acid positions on lipid nutrition. Nutr.Rev. 54: 108-110.

Delp, M. D. & Duan, C. (1996) Composition and size of type I, IIA, IID/X, and IIB fibers and citrate synthase activity of rat muscle. J Appl.Physiol 80: 261-270.

Delp, M. D., Manning, R. O., Bruckner, J. V. et al. (1991) Distribution of cardiac output during diurnal changes of activity in rats. Am.J.Physiol 261: H1487-H1493.

DeMar, J. C., Jr., DiMartino, C., Baca, A. W. et al. (2008) Effect of dietary docosahexaenoic acid on biosynthesis of docosahexaenoic acid from alpha-linolenic acid in young rats. J.Lipid Res. 49: 1963-1980.

Downward, K. (2004) Mass spectrometry: A foundation course The Royal Society of Chemistry, Cambridge.

Early, R. J. & Spielman, S. P. (1995) Muscle respiration in rats is influenced by the type and level of dietary fat. J.Nutr. 125: 1546-1553.

Emken, E. A. (2001) Stable isotope approaches, applications, and issues related to polyunsaturated fatty acid metabolism studies. Lipids 36: 965-973.

Evans, K., Burdge, G. C., Wootton, S. A. et al. (2002) Regulation of dietary fatty acid entrapment in subcutaneous adipose tissue and skeletal muscle. Diabetes 51: 2684-2690.

Fiehn, W., Peter, J. B., Mead, J. F. et al. (1971) Lipids and fatty acids of sarcolemma, sarcoplasmic reticulum, and mitochondria from rat skeletal muscle. J Biol.Chem 246: 5617-5620.

Fu, Z., Attar-Bashi, N. M., & Sinclair, A. J. (2001) 1-14C-linoleic acid distribution in various tissue lipids of guinea pigs following an oral dose. Lipids 36: 255-260.

Garda, H. A., Bernasconi, A. M., Tricerri, M. A. et al. (1997) Molecular species of phosphoglycerides in liver microsomes of rats fed a fat-free diet. Lipids 32: 507-513.

Gawrisch, K., Eldho, N. V., & Holte, L. L. (2003) The structure of DHA in phospholipid membranes. Lipids 38: 445-452.

Godin, J. P., Fay, L. B., & Hopfgartner, G. (2007) Liquid chromatography combined with mass spectrometry for 13C isotopic analysis in life science research. Mass Spectrom.Rev. 26: 751-774.

Gorski, J., Nawrocki, A., & Murthy, M. (1998) Characterization of free and glyceride-esterified long chain fatty acids in different skeletal muscle types of the rat. Mol.Cell Biochem. 178: 113-118.

Goto, J., Watanabe, K., Miura, H. et al. (1987) Studies on steroids. CCXXVIII Trace analysis of bile acids by gas chromatography-mass spectrometry with negative ion chemical ionization detection. J.Chromatogr. 388: 379-387.

Guo, Z. & Jensen, M. D. (1998) Intramuscular fatty acid metabolism evaluated with stable isotopic tracers. J.Appl.Physiol 84: 1674-1679.

Hamalainen, N. & Pette, D. (1995) Patterns of myosin isoforms in mammalian skeletal muscle fibres. Microsc.Res.Tech. 30: 381-389.

Han, X. X., Chabowski, A., Tandon, N. N. et al. (2007) Metabolic challenges reveal impaired fatty acid metabolism and translocation of FAT/CD36 but not FABPpm in obese Zucker rat muscle. Am.J.Physiol Endocrinol.Metab 293: E566-E575.

Harris, W. S., Miller, M., Tighe, A. P. et al. (2008) Omega-3 fatty acids and coronary heart disease risk: clinical and mechanistic perspectives. Atherosclerosis 197: 12-24.

Harrison, A. (1992) Chemical Ionization Mass Spectrometry CRC, Boca Raton.

Holloway, G. P., Luiken, J. J., Glatz, J. F. et al. (2008) Contribution of FAT/CD36 to the regulation of skeletal muscle fatty acid oxidation: an overview. Acta Physiol (Oxf) 194: 293-309.

Igarashi, M., Ma, K., Chang, L. et al. (2007) Dietary n-3 PUFA deprivation for 15 weeks upregulates elongase and desaturase expression in rat liver but not brain. J.Lipid Res. 48: 2463-2470.

Infante, J. P., Kirwan, R. C., & Brenna, J. T. (2001) High levels of docosahexaenoic acid (22:6n-3)-containing phospholipids in high-frequency contraction muscles of hummingbirds and rattlesnakes. Comp Biochem.Physiol B Biochem.Mol.Biol. 130: 291-298.

Jump, D. B. (2002) The biochemistry of n-3 polyunsaturated fatty acids. J.Biol.Chem. 277: 8755-8758.

Keizer, H. A., Schaart, G., Tandon, N. N. et al. (2004) Subcellular immunolocalisation of fatty acid translocase (FAT)/CD36 in human type-1 and type-2 skeletal muscle fibres. Histochem.Cell Biol. 121: 101-107.

Kiens, B., Roemen, T. H., & van der Vusse, G. J. (1999) Muscular long-chain fatty acid content during graded exercise in humans. Am.J.Physiol 276: E352-E357.

Kriketos, A. D., Pan, D. A., Sutton, J. R. et al. (1995) Relationships between muscle membrane lipids, fiber type, and enzyme activities in sedentary and exercised rats. Am.J Physiol 269: R1154-R1162.

Kuda, O., Jelenik, T., Jilkova, Z. et al. (2009) n-3 fatty acids and rosiglitazone improve insulin sensitivity through additive stimulatory effects on muscle glycogen synthesis in mice fed a high-fat diet. Diabetologia 52: 941-951.

Lambert, E. V., Speechly, D. P., Dennis, S. C. et al. (1994) Enhanced endurance in trained cyclists during moderate intensity exercise following 2 weeks adaptation to a high fat diet. Eur.J.Appl.Physiol Occup.Physiol 69: 287-293.

Laughlin, M. H. & Armstrong, R. B. (1983) Rat muscle blood flows as a function of time during prolonged slow treadmill exercise. Am.J.Physiol 244: H814-H824.

Lausevic, M., Plomley, J., Jiang, X. et al. (1995) Analysis of polychlorinated biphenyls by quadrupole ion trap mass spectrometry: Part I - Chemical ionization studies of co-eluting congeners 77 and 110. Eur.Mass Spectrom 1: 149-159.

Leaf, A. & Kang, J. X. (1996) Prevention of cardiac sudden death by N-3 fatty acids: a review of the evidence. J.Intern.Med. 240: 5-12.

Lin, Y. H., Pawlosky, R. J., & Salem, N., Jr. (2005) Simultaneous quantitative determination of deuterium- and carbon-13-labeled essential fatty acids in rat plasma. J.Lipid Res. 46: 1974-1982.

Lin, Y. H. & Salem, N., Jr. (2005) In vivo conversion of 18- and 20-C essential fatty acids in rats using the multiple simultaneous stable isotope method. J.Lipid Res. 46: 1962-1973.

Lin, Y. H. & Salem, N., Jr. (2007) Whole body distribution of deuterated linoleic and alpha-linolenic acids and their metabolites in the rat. J.Lipid Res. 48: 2709-2724.

Luiken, J. J., Miskovic, D., Arumugam, Y. et al. (2001) Skeletal muscle fatty acid transport and transporters. Int.J.Sport Nutr.Exerc.Metab 11 Suppl: S92-S96.

Luiken, J. J., Schaap, F. G., van Nieuwenhoven, F. A. et al. (1999) Cellular fatty acid transport in heart and skeletal muscle as facilitated by proteins. Lipids 34 Suppl: S169-S175.

MacLennan, D. H. & Holland, P. C. (1975) Calcium transport in sarcoplasmic reticulum. Annu.Rev.Biophys.Bioeng. 4: 377-404.

Masood, A., Stark, K. D., & Salem, N., Jr. (2005) A simplified and efficient method for the analysis of fatty acid methyl esters suitable for large clinical studies. J.Lipid Res. 46: 2299-2305.

Masood, M. A. & Salem, N., Jr. (2008) High-throughput analysis of plasma fatty acid methyl esters employing robotic transesterification and fast gas chromatography. Lipids 43: 171-180.

McCloy, U., Ryan, M. A., Pencharz, P. B. et al. (2004) A comparison of the metabolism of eighteen-carbon 13C-unsaturated fatty acids in healthy women. J.Lipid Res. 45: 474-485.

McMurchie, E. J. (1988) Dietary lipids and regulation of membrane fluidity. In: Physiological Regulation of Membrane Fluidity (Aloia, R. C., Curtain, C. C., & Gordon, L. M., eds.), pp. 189-237. Advances in membrane fluidity, vol. 3, Alan R. Liss, New York.

Miller, W. C., Bryce, G. R., & Conlee, R. K. (1984) Adaptations to a high-fat diet that increase exercise endurance in male rats. J.Appl.Physiol 56: 78-83.

Morimoto, K. C., Van Eenennaam, A. L., DePeters, E. J. et al. (2005) Endogenous production of n-3 and n-6 fatty acids in mammalian cells. J.Dairy Sci. 88: 1142-1146.

Morrison, W. R. & Smith, L. M. (1964) Preparation of fatty acid methyl esters and dimethylacetals from lipids with boron fluoride-methanol. J.Lipid Res. 4: 600-608.

Muoio, D. M., Leddy, J. J., Horvath, P. J. et al. (1994) Effect of dietary fat on metabolic adjustments to maximal VO2 and endurance in runners. Med.Sci.Sports Exerc. 26: 81-88.

Murphy, M. G. (1990) Dietary fatty acids and membrane protein function. J.Nutr.Biochem. 1: 68-79.

Nakamura, M. T., Cho, H. P., Xu, J. et al. (2001) Metabolism and functions of highly unsaturated fatty acids: an update. Lipids 36: 961-964.

Nickerson, J. G., Momken, I., Benton, C. R. et al. (2007) Protein-mediated fatty acid uptake: regulation by contraction, AMP-activated protein kinase, and endocrine signals. Appl.Physiol Nutr.Metab 32: 865-873.

Nikolaidis, M. G., Petridou, A., & Mougios, V. (2006) Comparison of the phospholipid and triacylglycerol fatty acid profile of rat serum, skeletal muscle and heart. Physiol Res. 55: 259-265.

Noy, N., Donnelly, T. M., & Zakim, D. (1986) Physical-chemical model for the entry of water-insoluble compounds into cells. Studies of fatty acid uptake by the liver. Biochemistry 25: 2013-2021.

Oscai, L. B., Essig, D. A., & Palmer, W. K. (1990) Lipase regulation of muscle triglyceride hydrolysis. J.Appl.Physiol 69: 1571-1577.

Pawlosky, R. J., Sprecher, H. W., & Salem, N., Jr. (1992) High sensitivity negative ion GC-MS method for detection of desaturated and chain-elongated products of deuterated linoleic and linolenic acids. J.Lipid Res. 33: 1711-1717.

Pette, D. & Staron, R. S. (1990) Cellular and molecular diversities of mammalian skeletal muscle fibers. Rev.Physiol Biochem.Pharmacol. 116: 1-76.

Pudelkewicz, C., Seufert, J., & Holman, R. T. (1968) Requirements of the female rat for linoleic and linolenic acids. J.Nutr. 94: 138-146.

Ranvier, L. (1873) Propriétes et structures différentes des muscles rouges et des muscles blanc, chez les lapins et chez les raises. C R hepd Séanc Acad Sci (Paris) 77: 1030-1043.

Rossmeisl, M., Jelenik, T., Jilkova, Z. et al. (2009) Prevention and reversal of obesity and glucose intolerance in mice by DHA derivatives. Obesity.(Silver.Spring) 17: 1023-1031.

Sahlin, K., Edstrom, L., Sjoholm, H. et al. (1981) Effects of lactic acid accumulation and ATP decrease on muscle tension and relaxation. Am.J.Physiol 240: C121-C126.

Salem, N., Jr., Reyzer, M., & Karanian, J. (1996) Losses of arachidonic acid in rat liver after alcohol inhalation. Lipids 31 Suppl: S153-S156.

Samuelsson, B. (1983) From studies of biochemical mechanism to novel biological mediators: prostaglandin endoperoxides, thromboxanes, and leukotrienes. Nobel Lecture, 8 December 1982. Biosci.Rep. 3: 791-813.

SanGiovanni, J. P., Berkey, C. S., Dwyer, J. T. et al. (2000) Dietary essential fatty acids, long-chain polyunsaturated fatty acids, and visual resolution acuity in healthy fullterm infants: a systematic review. Early Hum.Dev. 57: 165-188.

Schiaffino, S. & Reggiani, C. (1994) Myosin isoforms in mammalian skeletal muscle. J.Appl.Physiol 77: 493-501.

Schmidt, A., Wolde, M., Thiele, C. et al. (1999) Endophilin I mediates synaptic vesicle formation by transfer of arachidonate to lysophosphatidic acid. Nature 401: 133-141.

Sheaff, R. C., Su, H. M., Keswick, L. A. et al. (1995) Conversion of alpha-linolenate to docosahexaenoate is not depressed by high dietary levels of linoleate in young rats: tracer evidence using high precision mass spectrometry. J.Lipid Res. 36: 998-1008.

Shimada, Y., Morita, T., & Sugiyama, K. (2003) Dietary eritadenine and ethanolamine depress fatty acid desaturase activities by increasing liver microsomal phosphatidylethanolamine in rats. J.Nutr. 133: 758-765.

Shimura, T., Miura, T., Usami, M. et al. (1997) Docosahexanoic acid (DHA) improved glucose and lipid metabolism in KK-Ay mice with genetic non-insulin-dependent diabetes mellitus (NIDDM). Biol.Pharm.Bull. 20: 507-510.

Simi, B., Sempore, B., Mayet, M. H. et al. (1991) Additive effects of training and high-fat diet on energy metabolism during exercise. J.Appl.Physiol 71: 197-203.

Smerdu, V., Karsch-Mizrachi, I., Campione, M. et al. (1994) Type IIx myosin heavy chain transcripts are expressed in type IIb fibers of human skeletal muscle. Am.J.Physiol 267: C1723-C1728.

Smol, E., Zernicka, E., Czarnowski, D. et al. (2001) Lipoprotein lipase activity in skeletal muscles of the rat: effects of denervation and tenotomy. J.Appl.Physiol 90: 954-960.

Spangenburg, E. E. & Booth, F. W. (2003) Molecular regulation of individual skeletal muscle fibre types. Acta Physiol Scand. 178: 413-424.

Stark, K. D., Lim, S. Y., & Salem, N., Jr. (2007) Docosahexaenoic acid and n-6 docosapentaenoic acid supplementation alter rat skeletal muscle fatty acid composition. Lipids Health Dis. 6: 13.

Staron, R. S. & Pette, D. (1986) Correlation between myofibrillar ATPase activity and myosin heavy chain composition in rabbit muscle fibers. Histochemistry 86: 19-23.

Stubbs, C. D. & Smith, A. D. (1984) The modification of mammalian membrane polyunsaturated fatty acid composition in relation to membrane fluidity and function. Biochim.Biophys.Acta 779: 89-137.

Su, H. M., Corso, T. N., Nathanielsz, P. W. et al. (1999) Linoleic acid kinetics and conversion to arachidonic acid in the pregnant and fetal baboon. J.Lipid Res. 40: 1304-1312.

Thomson, A. B., Keelan, M., Garg, M. L. et al. (1989) Intestinal aspects of lipid absorption: in review. Can.J.Physiol Pharmacol. 67: 179-191.

Varian, Inc. Mass Spectrometry WorkStation Version 6: 4000 MS mannual. 2006.
Ref Type: Catalog

Voet, D. & Voet, J. G. (2004) Biochemistry John Wiley & Sons, New York.

Waki, H., Watanabe, K., Ishii, H. et al. (2004) Whole-body β-oxidation of docosahexaenoic acid is decreased under n-3 polyunsaturated fatty acid insufficiency as assessed by $^{13}CO_2$ breath test using [U-^{13}C] fatty acids. J.Oleo.Sci. 53: 135-142.

Wanders, R. J. & Waterham, H. R. (2006) Biochemistry of mammalian peroxisomes revisited. Annu.Rev.Biochem. 75: 295-332.

Weithmann, K. U., Peterson, H., & Sevanian, A. (1989) Incorporation of arachidonic, dihomogamma linolenic and eicosapentaenoic acids into cultured V79 cells. Lipids 24: 173-178.

Wheeler, K. P., Walker, J. A., & Barker, D. M. (1975) Lipid requirement of the membrane sodium-plus-potassium ion-dependent adenosine triphosphatase system. Biochem.J. 146: 713-722.